Earth-Science Reviews 192 (2019) 337–354

Contents lists available at ScienceDirect

Earth-Science Reviews

journal homepage: www.elsevier.com/locate/earscirev

Westerlies Asia and monsoonal Asia: Spatiotemporal differences in climate change and possible mechanisms on decadal to sub-orbital timescales

Fahu Chen[a,b,*,1], Jianhui Chen[a,1], Wei Huang[a,1], Shengqian Chen[a], Xiaozhong Huang[a], Liya Jin[a], Jia Jia[a], Xiaojian Zhang[a], Chengbang An[a], Jiawu Zhang[a], Yan Zhao[c], Zicheng Yu[d], Renhe Zhang[e], Jianbao Liu[a,b], Aifeng Zhou[a], Song Feng[f]

[a] Key Laboratory of Western China's Environmental Systems (Ministry of Education), College of Earth and Environmental Sciences, Lanzhou University, Lanzhou 730000, China
[b] Key Laboratory of Alpine Ecology (LAE), CAS Center for Excellence in Tibetan Plateau Earth Sciences, Institute of Tibetan Plateau Research, Chinese Academy of Sciences (CAS), Beijing 100101, China
[c] Institute of Geographic Sciences and Natural Resources Research, Chinese Academy of Sciences (CAS), Beijing 100101, China
[d] Department of Earth and Environmental Sciences, Lehigh University, Bethlehem, PA 18015, USA
[e] Institute of Atmospheric Sciences, Fudan University, Shanghai 200433, China
[f] Department of Geosciences, University of Arkansas, Fayetteville, AR 72701, USA

ARTICLE INFO

Keywords:
Holocene
Westerlies Asia and Monsoonal Asia
Westerlies-dominated climatic regime (WDCR)
Core area of WDCR
Silk Road pattern (SRP)

ABSTRACT

The 'westerlies-dominated climatic regime' (WDCR) in the present interglacial period was proposed because precipitation/moisture variations between arid central Asia and mid-latitude monsoonal Asia are out-of-phase or anti-phased on different timescales during the Holocene. In this study. we first review the development of the theoretical framework of the WDCR, and then outline the boundary of its core area: from the Caspian Sea in the west to the western Hexi Corridor in the east, with the northern and southern limits coinciding with the domain of arid central Asia. Next, we present a synthesis of multiple lines of evidence for the occurrence of the WDCR on multi-millennial ('sub-orbital' herein) to decadal timescales during the Holocene. Finally, we examine the possible physical mechanisms responsible for the WDCR. We find that external factors (insolation changes induced by orbital factors) generated the WDCR on a sub-orbital timescale, whereas a circum-global teleconnection/Silk Road pattern was the most significant factor responsible for the WDCR on centennial and decadal timescales. The study provides a comprehensive summary of the development of our knowledge of the WDCR over the past several decades, together with a tentative theoretical framework for understanding climatic and environmental changes within its region of influence. In addition, it forms a scientific basis for environmental management and ecological restoration in this arid region in the context of global warming.

1. Introduction

From the perspective of the dominant atmospheric circulation systems, Asia can be roughly divided into two main regions: 'Westerlies Asia' (i.e. arid central Asia composed of NW China and Central Asia) and 'Monsoonal Asia' (i.e. eastern and southern Asia) (Li, 1990; Herzschuh, 2006; Chen et al., 2008; An et al., 2012; Wang et al., 2017; Chen et al., 2018). Early works in the 1990s highlighted the differences between the NW arid region and the SE monsoonal region in China in terms of their patterns of climate change both at the orbital timescale since the last interglacial, and on sub-orbital timescale within the last glacial period. Based on the limited dating technologies and paleoenvironmental proxies available at that time, it was suggested that the climatic associations of 'cold and wet' or 'warm and dry' occurred in NW China (Li, 1990; Han and Qu, 1992; Han et al., 1993), in contrast with the 'cold and dry' or 'warm and wet' patterns of the monsoon climate, during the last glacial/interglacial cycle. However, it was recently found that the Chashmanigar loess–paleosol sequence from southern Tajikistan (38.4°N, 69.8°E) in Central Asia is well correlated for the past 1.77 Myr with the Lingtai loess-paleosol sequence (35.0°N,

* Corresponding author at: Key Laboratory of Western China's Environmental Systems (Ministry of Education), College of Earth and Environmental Sciences, Lanzhou University, Lanzhou 730000; Key Laboratory of Alpine Ecology (LAE), CAS Center for Excellence in Tibetan Plateau Earth System Sciences, Institute of Tibetan Plateau Research, Chinese Academy of Sciences (CAS), Beijing 100101, China.
E-mail addresses: fhchen@lzu.edu.cn, fhchen@itpcas.ac.cn (F. Chen).
[1] These authors contributed equally to this work.

https://doi.org/10.1016/j.earscirev.2019.03.005
Received 23 February 2018; Received in revised form 5 March 2019; Accepted 5 March 2019
Available online 11 March 2019
0012-8252/ © 2019 Elsevier B.V. All rights reserved.

107.5°E) from the Chinese Loess Plateau - with loess being deposited during cold and dry glacial periods, and paleosols forming during warm and wet interglacial periods (Ding et al., 2002; Yang et al., 2006a). This work implied that climate changes in westerlies Asia may be consistent with those in monsoonal Asia on orbital timescales over glacial/interglacial cycles. Furthermore, although early works showed that a humid climate and relatively high lake levels occurred during the Last Glacial Maximum (LGM, 26.5–19/18 ka (1 ka = 1000 cal yr BP); Clark et al., 2009) in Xinjiang Province in China (Li, 1990; Yu et al., 2000), most of the recent studies have argued that the arid central Asia experienced a dry climate, with sparse vegetation cover and relatively low lake levels (e.g. An et al., 2013; Zhao et al., 2015; Li et al., 2016) - in other words synchronous with the climatic conditions in the monsoon region on the sub-orbital timescale at that time (e.g. Kuang et al., 2013; Cui et al., 2015).

With regard to climate change over arid central Asia during the present Holocene interglacial, numerous paleo-moisture records based on better dating and more reliable proxies have been published since about 2000 AD (e.g. Boomer et al., 2000; Ricketts et al., 2001; Fowell et al., 2003; Wick et al., 2003; Herzschuh et al., 2004; Wang et al., 2004; Jiang et al., 2007; Huang et al., 2009). Chen et al. (2008, 2009a) synthesized 12 high-quality lake sediments records and found that this region experienced a dry climate during the early Holocene, and that most lakes only appeared after ~7–8 ka, with high lake levels and a more humid climate during the mid- and late Holocene. This finding is supported by a recent review based on pollen records (Wang and Feng, 2013). Therefore, not only NW China, but also Central Asia, experienced a different pattern of Holocene climate change to that of the monsoonal region, with the latter generally following changes in Northern Hemisphere summer insolation (NHSI) (Fleitmann et al., 2007; Chen et al., 2014a; Chen et al., 2015a). Naturally, the moisture variations in the arid region cannot be explained using the traditional concept of the penetration of the summer monsoon further inland (e.g. Wei and Gasse, 1999; Feng et al., 2006).

In addition, changes in the moisture status of the arid central Asia differ from those of monsoonal Asia on centennial to millennial timescales. For example, precipitation increased in the major mountain ranges of NW China, such as the Western Kunlun Mountains (Yao et al., 1996), Qilian Mountains (Liu et al., 1998), and Tienshan Mountains (Chen et al., 2006) during the Little Ice Age (LIA; 1400–1900 CE). Lake levels or fluvial discharges increased in the major basins such as the southern Tarim Basin (Liu, 1976; Yang et al., 2002), the Juyan Lake Basin of the Alxa Plateau (Zhang et al., 1998), the Dzungar Basin (Wu et al., 2004), and the Qaidam Basin (Chen et al., 2009b). All this evidence demonstrates that NW China experienced a relatively wet climate at that time (Chen et al., 2010). By contrast, studies of various archives, including stalagmites (Zhang et al., 2008; Tan et al., 2011), tree rings (Linderholm and Braeuning, 2006), deep-sea sediments (Anderson et al., 2002), and historical documents (Zheng et al., 2006), as well as numerical simulations (Zhou et al., 2011; Huang et al., 2018), all indicate that the Asian monsoon was relatively weak, at least during the first half of the LIA, and was gradually enhanced after the mid- to late 17th century.

On the decadal timescale, Shi et al. (2007) asserted that since the late 1980s the climate of NW China began to change from a ‘warm and dry’ pattern to a ‘warm and wet’ pattern. Modern observational data also show an increase in precipitation and moisture in the inland arid region over the past several decades (Ma and Fu, 2006; Feng et al., 2007; Jiang et al., 2009; Chen et al., 2011; Huang et al., 2013). Concurrently, the decline of the Asian monsoon (Li and Zeng, 2003; Wang and Ding, 2006; Ding et al., 2008) has resulted in the large-scale aridification of North China (Ma and Fu, 2006) and substantially decreased precipitation in the monsoon boundary region (Jin et al., 2005; Qian and Qin, 2008).

The foregoing studies indicate that moisture and precipitation changes in arid central Asia, climatologically controlled by the westerlies, differed significantly from those of monsoonal Asia (mainly mid-latitude monsoonal Asia) on different timescales during the Holocene. Therefore, we have proposed the theoretical framework of a ‘westerlies-dominated climatic regime’ (WDCR) for moisture changes (Chen et al., 2008; Chen et al., 2009a, 2010).

The increasing interest in the paleoclimatic and paleoenvironmental record of arid central Asia (e.g. Holmes et al., 2009; Yang et al., 2009; Li et al., 2011a; Mischke and Zhang, 2011; Feng et al., 2013; Hong et al., 2014; Song et al., 2015; Cheng et al., 2016; Cai et al., 2017) makes it necessary to systematically review and integrate the available evidence for the existence of the WDCR on various timescales during the Holocene, and such a synthesis is important for assessing the newly-developed proxy records and for exploring the spatial extent of this climatic regime. Furthermore, two important questions are the nature of the underlying physical mechanisms of the WDCR, and whether these physical mechanisms vary on different timescales. The present study seeks to address these research issues by presenting a comprehensive compilation and synthesis of the available data and knowledge. The paper is structured as follows: Section 2 defines the core region of the WDCR; Sections 3–5 discuss the evidence for the existence of the WDCR on different timescales during the Holocene, together with its spatial extent; and Section 6 proposes several driving mechanisms of the WDCR. The overall objective is to shed more light on the possible climatic and environmental responses in arid central Asia to global warming, and to promote the development of a theoretical framework for understanding climatic and environmental changes in the region.

2. Overview of Westerlies Asia and Monsoonal Asia

The modern northern limit of the Asian summer monsoon can be regarded as the approximate boundary between westerlies Asia (or the westerlies region) and monsoonal Asia (or the monsoonal region) (Fig. 1; Chen et al., 2009a). Westerlies Asia is on the western side of mid-latitude Asia, and its extent is essentially equivalent to arid central Asia (see the orange dashed lines in Fig. 1). The region is characterized by an arid climate, a landscape with sparse vegetation cover, and a fragile ecological environment. Westerlies Asia comprises a unique mountain–basin structure and associated distinct vertical zonation consisting of ice and snow, alpine meadow, forest, grassland, oases, and desert. Among these landscapes, the mountain and plateau areas have relatively abundant precipitation, which are the major water resources for the region, providing most of the water that underpins the economy of the Silk Road and the development of oases.

Mid-latitude arid central Asia, the world's largest azonal arid region, differs significantly from other major arid regions in the subtropics. Climate change in this region is primarily influenced by the intensity and location of the westerlies circulation (Fig. 1) (Rogers and Van, 1979; Aizen et al., 2001; Huang et al., 2013). The large amount of atmospheric dust aerosols emitted from the region, in turn, has a significant effect on the global climate (Uno et al., 2009). While across monsoonal Asia, the Indian monsoon and East Asian monsoon supply abundant rainfall in summer, resulting in a significantly wetter climate than in winter. Horizontal zonation develops along the direction of the advancing summer monsoon and precipitation is mainly controlled by the intensity of the monsoon circulation (Wang, 2001; Xiao et al., 2004; Shen et al., 2005; Wang et al., 2005; Wang and Chen, 2012; Liu et al., 2014).

Given that the Asian summer monsoon barely reaches arid central Asia, initial studies of the WDCR (e.g. Chen et al., 2008, 2009b) considered this entire region to investigate the spatiotemporal contrasts with monsoonal Asia with respect to precipitation/moisture variations. Recently, the a 9-year low-pass filter was applied to the summer precipitation data over mid-latitude Eurasia (30–60°N, 0–130°E) during 1960–2010 to analyses decadal variations of summer precipitation using EOF method. The results suggested that the WDCR during the instrumental period is most significant on decadal timescales in

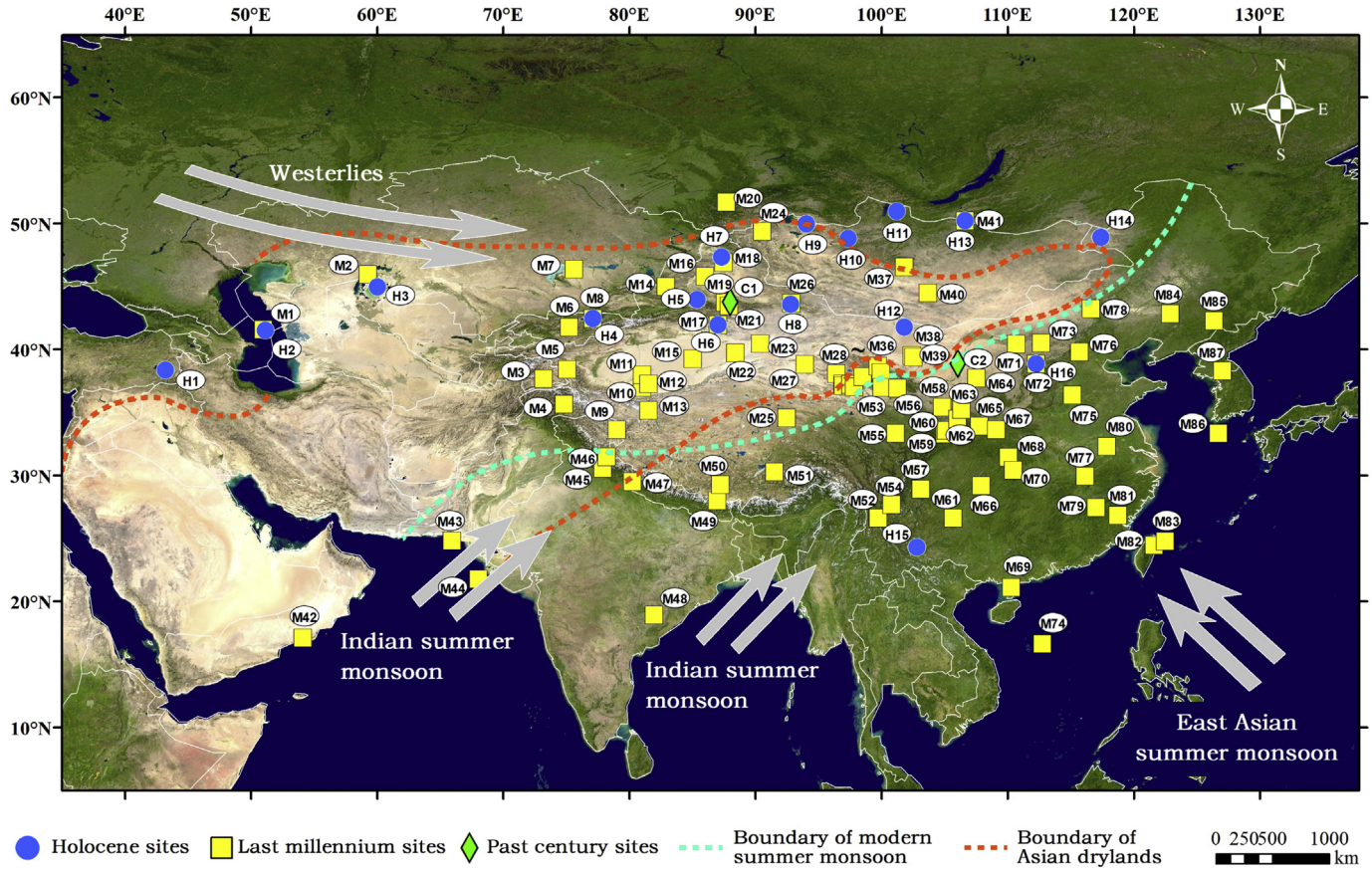

Fig. 1. Locations of proxy records of paleo-precipitation/moisture changes over different timescales (H1-H16 for Holocene sites, M1-M87 for last millennium sites, and C1-C2 for past century sites). The green dashed line indicates the modern limit of the summer monsoon (after Chen et al., 2008a; Chen et al., 2009a); the area enclosed by the orange dashed line is arid central Asia (modified from Feng and Fu, 2013). See Table 1 for details of these proxy records. (For interpretation of the references to colour in this figure legend, the reader is referred to the web version of this article.)

summer. Decadal summer precipitation variations in a sub-region of westerlies Asia were the opposite to those of the mid-latitude East Asian monsoon region (in the east) and the Mediterranean area (in the west) during the past 50 years. Therefore, this sub-region in westerlies Asia is subsequently referred to as the core area of the WDCR (the region enclosed by the red dashed lines in Fig. 2). The boundaries of the core area of the WDCR are as follows: the Caspian Sea (approximately 50°E) to the west, the western Hexi Corridor (approximately 90°E) to the east, and the southern and northern limits of arid central Asia to the south and north (approximately 36–54°N) (Huang et al., 2015a). Geographically, the region is roughly equivalent to Central Asia and Xinjiang Province in China.

The above definition enables us to better demonstrate the spatial pattern of climate changes over mid-latitude Asia. First, the core area of the WDCR is in the central and western parts of arid central Asia and its climate is dominated by the westerlies circulation; in other words, it is the part of arid central Asia that is largely unaffected by the advance and retreat of the summer monsoon on annual, decadal or longer timescales. The patterns of climate change of this region are unique in mid-latitude Eurasia. Second, for the mid-latitude East Asian monsoon region and Eastern Mongolia, precipitation and moisture changes are overwhelmingly dominated by the summer monsoon circulation. Third, there is a transitional belt inbetween these two regions (the green dashed lines in Fig. 2) that is influenced by both the westerlies and monsoon system, resulting in an even more complex pattern of climate change. In addition, it should be noted that the areal extents of the core area of the WDCR, the transitional zone, and the mid-latitude East Asian monsoon region may vary on different timescales, depending on the changing intensities of the summer monsoon and westerlies, as well as on their relative strengths.

3. Trend in moisture changes on a sub-orbital scale during the Holocene

We previously collected and synthesized records of Holocene moisture changes from 12 lakes (H1, H3, H4, H6-H14 in Fig. 1) with reliable chronologies and robust proxies, and calculated the average effective moisture for arid central Asia (Chen et al., 2008, 2009a). The results showed that during the early Holocene, most of these lakes were dry or at a low level. During the mid-Holocene (8–4 ka), the lakes experienced maxima in effective moisture. Moisture then declined during the late Holocene, but it was still higher than that during the early Holocene (Fig. 3b). This result led us to propose the westerlies-dominated climatic regime, and we suggested that the pattern of moisture variations in arid central Asia differed from that of mid-latitude monsoonal Asia, exhibiting an 'out-of-phase' relationship. It is worth noting that our WDCR proposition on the sub-orbital timescale is distinctly different from the earlier hypothesis that climate changes within arid central Asia are asynchronous with those of the Asian monsoon region on a glacial-interglacial timescale (e.g. Han and Qu, 1992). Also, as mentioned in Section 1, the wet LGM climate of Xinjiang Province identified in the earlier studies is currently considered problematic because of dating uncertainties and limited proxies. There is a growing consensus that, during the glacial period, the climate changes in the westerlies region are consistent with those in the monsoonal region of China at the sub-orbital timescale (e.g. Zhao et al., 2015; Li et al.,

Table 1
Paleo-precipitation/moisture records used in this study (updated from Chen et al., 2008, Chen et al., 2015b).

Site no.	Site name	Lat. (°N)	Long. (°E)	Time period (cal BP)	Sample resolution (yr)[a]	Dating material	Dating method	No. of dates[b]	Proxies used[c]	Proxy indication	References
H1	Lake Van	38.40	43.20	ca. 13,700–0	20	–	Varve counting	–	$\delta^{18}O$, pollen, sediment deposition rate	River discharge, moisture	Landmann et al. (1996); Wick et al. (2003)
H2	Caspian Sea	41.55	51.10	ca. 12,400–2400	110	Ostracods	^{14}C	4/6	Pollen	Moisture	Leroy et al. (2014)
H3	Aral Sea	45.00	60.00	ca. 12,000–0	200	TOC (total organic carbon), molluscs, terrestrial macrofossils, *Vaucheria* sp.	^{14}C	12	Terrace, historical documents, sediment deposition rate, $CaCO_3$	Lake level (river discharge)[d]	Boomer et al. (2000)
H4	Issyk-Kul	42.50	77.10	ca. 8000–0	195	Bulk sediment	^{14}C	8	$\delta^{18}O$, $CaCO_3$, pollen	Lake level (river discharge), moisture	Rasmussen et al. (2001); Ricketts et al. (2001); Ferronskii et al. (2003)
H5	Yili River valley	43.97	85.34	ca. 16,700–0	100	Quartz and K-feldspar	OSL	21/24	Magnetic susceptibility	Moisture	Chen et al. (2016a)
H6	Bosten Lake	42.00	87.02	ca. 17,000–0	10	TOC, terrestrial plant macrofossil, plant, tree leaves, organic matter, quartz	^{14}C, OSL	16/18	Pollen, grain size, $CaCO_3$	Lake level, moisture	Wünnemann et al. (2003, 2006); Huang (2006); Huang et al. (2009)
H7	Wulungu Lake	47.20	87.29	ca. 9600–0	45	TOC	^{14}C	6	Grain size, pollen	Precipitation, lake level, water depth, effective moisture	Liu et al. (2008)
H8	Balikun Lake	43.62	92.77	ca. 16,700–0	65	Organic matter, plant macrofossils, pollen	^{14}C	12/13	Pollen	Effective moisture	Tao et al. (2010)
H9	Bayan Nuur	50.00	94.02	ca. 15,600–0	–	Organic sediment, limnohumite, wood,	^{14}C	7/11	Terraces, pollen	Moisture, lake level	Dorofeyuk and Tarasov (1998); Grunert et al. (2000)
H10	Telmen Lake	48.83	97.33	ca. 7000–0	190	Pollen, bulk sediment	^{14}C	6	Diatom, pollen, $CaCO_3$	Effective moisture	Peck et al. (2002); Fowell et al. (2003)
H11	Hovsgol Nuur	51.00	101.20	ca. 14,500–0	200	TOC, plant	^{14}C	10	Diatom, pollen, biogenic silica, magnetic susceptibility	Lake level, precipitation	Tarasov et al. (1996); Dorofeyuk and Tarasov (1998); Karabanov et al. (2004); Nara et al. (2005); Prokopenko et al. (2005)
H12	Juyan Lake	41.80	101.8	ca. 10,700–0	160	Organic matter	^{14}C	5	Pollen	Precipitation, moisture	Chen et al. (2003); Herzschuh et al. (2004)
H13	Gun Nuur	50.25	106.60	ca. 9400–0	25	Bulk sediment	^{14}C	9	Diatom, $\delta^{13}Corg$, $CaCO_3$, magnetic susceptibility	Lake level, moisture	Wang et al. (2004); Feng et al. (2005)
H14	Hulun Nuur	48.92	117.38	ca. 12,000–0	150	–	^{14}C	6	Pollen, magnetic susceptibility	Moisture, lake level	Wang and Ji (1995); Yang and Wang (1996)
H15	Xingyun Lake	24.34	102.78	ca. 9500–0	230	Plants remains, charcoal	^{14}C	8	Pollen	Precipitation	Chen et al. (2014a)
H16	Gonghai Lake	38.90	112.23	ca. 14,700–0	20	Terrestrial plant macrofossil	^{14}C	20/25	Pollen	Precipitation	Chen et al. (2015a)
M1	Caspian Sea	41.62	50.95	Dis.[e]	–	Mollusc specimens	^{14}C	2	Barrier complex	Lake level (river discharge)	Kroonenberg et al. (2007)
				Dis.	–	Didacna, cardium, peat, Gastropoda, shells	^{14}C	23	Sand bar and bays	Lake level	Karpychev (2001)
M2	Aral Sea	45.00	60.00	ca. 1800–0	15	Filamentous green alga *Vaucheria* sp., TOC, $CaCO_3$ of mollusc shell.	^{137}Cs, ^{14}C	4/9	Reworked dinoflagellate cysts	Sheet wash (precipitation)	Sorrel et al. (2006)
M3	Sasikul Lake	37.70	73.18	ca. 2500–0	20	Bulk organic matter	^{210}Pb, ^{137}Cs, ^{14}C	3/6	$\delta^{18}O_{carb}$, TIC (total inorganic carbon)	Effective moisture (precipitation)	Lei et al. (2014)
M4	Northern Pakistan	35.70	74.80	1050–0	1	–	Ring counting	–	Tree-ring $\delta^{18}O$	Precipitation	Treydte et al. (2006)
M5	Karakuli Lake	38.44	75.06	ca.4200–0	30	TOC	$^{210}Pb/^{137}Cs$, ^{14}C	6/17	δD, $\delta^{13}C$	Effective moisture	Aichner et al. (2015)
M6	Son Kol Lake	41.80	75.20	ca.6000–0	50	Bulk sediment, shells, terrestrial plant remains	^{241}Am, ^{14}C	1/23	δD, $\delta^{15}N$	Summer moisture and winter snowfall	Lauterbach et al. (2014)
M7	Balkhash Lake	46.40	75.60	ca. 2500–0	10	Bulk sediment	^{14}C	9/17	Pollen	Moisture	Feng et al. (2013)

(*continued on next page*)

Table 1 (*continued*)

Site no.	Site name	Lat. (°N)	Long. (°E)	Time period (cal BP)	Sample resolution (yr)[a]	Dating material	Dating method	No. of dates[b]	Proxies used[c]	Proxy indication	References
M8	Issyk-kul Lake	42.50	77.10	Dis.	–	–	History	–	Historical map	Lake level (precipitation)	Narama et al. (2010)
M9	Bangongcuo Lake	33.67	79.00	ca. 11,400–0	70	$CaCO_3$, ostracods, TOC, shells, aquatic plants	^{14}C	0/11	$\delta^{18}O_{carb}$	Moisture	Wei and Gasse (1999); Fontes et al. (1996)
M10	Cele County	37.00	81.00	ca. 4000–0	40	Organic matter	^{14}C	3/6	Pollen, element composition	Moisture	Zhong and Xiong (1999)
M11	Southern Tarim rivers	38.00	81.00	Dis.	–	–	History	–	Historical documents	River discharge	Liu (1976)
M12	Keriya River	37.30	81.50	Dis.	–	*Populus* leaves	^{14}C	4	Terrace, historical documents	Fluvial environment (precipitation)	Yang et al. (2002); Yang et al. (2006b)
M13	Guliya ice cap	35.20	81.50	ca. 1700–0	10	–	Annual layer counting, ice flow model	–	Net accumulation rate	Precipitation	Yao et al. (1996); Thompson et al. (1995)
M14	Aibi Lake	45.02	82.86	ca. 13,900–0	10	Bulk sediment	^{14}C	3/6	Pollen	Moisture	Wang et al. (2013a)
M15	Tarim Basin	39.29	85.01	Dis.	–	Organic matter	^{14}C	42	Chronology of subfossil trees, reeds and mollusks	Groundwater level	Putnam et al. (2016)
M16	Manas Lake	45.83	85.97	ca.1000–0	5	Organic matter, plant	^{210}Pb, ^{137}Cs, ^{14}C	6	C_{37}, magnetic susceptibility, lightness,Ca	Lake level (effective moisture)	Song et al. (2015)
M17	Bosten Lake	42.00	87.02	ca. 1000–0	10	TOC, plant remains	^{210}Pb, ^{137}Cs, ^{14}C	2	Carbonate content, grain size, pollen	Effective moisture, precipitation	Chen et al. (2006)
M18	Jili Lake	46.93	87.42	ca. 2500–0	50	TOC	^{210}Pb, ^{137}Cs, ^{14}C	2	Grain size	Precipitation/lake level	Jiang et al. (2010)
M19	Central Tianshan Mountains	43.77	87.58	ca. 4500–0	70	–	^{14}C	1	Pollen	Moisture	Zhang et al. (2009)
M20	Teletskoye Lake	51.72	87.66	ca. 800–0	1	Plant remains	^{137}Cs, ^{14}C	2	Element composition, X-ray density	Precipitation, moisture	Kalugin et al. (2007)
M21	Chaiwobu Peatland	43.50	87.90	ca. 8500–0	25	Peat	^{14}C	3/19	Cellulose $\delta^{13}C$	Precipitation	Hong et al. (2014)
M22	Eastern fringe of Tarim Basin	39.78	88.39	ca. 800–0	4	Plant remains	^{14}C	5	Plant $\delta^{13}C$	Moisture	Liu et al. (2010)
M23	Luobupo Lake	40.47	90.35	ca. 15,300–0	40	Organic carbon	^{14}C	1	Grain size, microbiological and geochemical data	Lacustrine environment (precipitation)	Ma et al. (2008)
M24	Achit Nuur	49.42	90.52	ca. 22,600–0	50	Bulk sediment, mollusc	^{14}C	3/10	Pollen	Precipitation	Sun et al. (2013)
M25	Goulucuo Lake	34.60	92.47	ca. 1000–0	10	Bulk sediment	^{210}Pb, ^{137}Cs	1	Carbonate content	Effective moisture	Li et al. (2004)
M26	Balikun Lake	43.70	92.83	ca. 9400–0	75	TOC	^{14}C	2/7	$\delta^{18}O_{carb}$, TOC	Effective moisture	Xue and Zhong (2011)
M27	Sugan Lake	38.85	93.90	ca. 1000–0	10	–	Varve counting	–	Chironomid, $\delta^{18}O_{carb}$	Salinity (Effective moisture)	Chen et al. (2009b)
M28	Dunde ice cap	38.10	96.40	ca. 12,000–0	100	–	Annual layer counting, ice flow model	–	Pollen	Moisture	Liu et al. (1998)
M29	Hurleg Lake	37.28	96.90	ca. 1700–0	15	Plant macrofossils	^{210}Pb, ^{137}Cs, ^{14}C	5/6	Pollen	Effective moisture	Zhao et al. (2010)
M30	Toson Lake	37.14	96.94	ca. 1100–0	1	Plant macrofossils	^{14}C	3/4	Rb/Sr, Ca/Ti, TOC	Moisture	Ling et al. (2018)
M31	Gahai Lake	37.13	97.52	ca. 2600–0	6	Bulk organic matter	^{14}C	1/4	%C37:4	Moisture	He et al. (2013a)
M32	Delingha	37.27	97.53	1010-(−50)	3	–	Ring counting	–	Tree-ring $\delta^{18}O$	Relative moisture	Wang et al. (2013b)
M33	Zongwulong and Shalike Mts	37.08	97.82	1000-(−50)	1	–	Ring counting	–	Tree-ring width	Precipitation	Shao et al. (2005)
M34	NE Tibetan Plateau	37.85	98.50	3500–0	1	–	Ring counting	–	Tree-ring width	Precipitation	Yang et al. (2014)
M35	Middle Qilian Mountains	38.70	99.69	1230-(−50)	1	–	Ring counting	–	Tree-ring width	Precipitation	Zhang et al. (2011)
M36	Heihe River Basin	38.18	99.94	1500–0	1	–	Ring counting	–	Tree-ring width	River runoff	Yang et al. (2012)
M37	Khuisiin Lake	46.60	101.80	ca. 1200–0	20	–	^{210}Pb, ^{137}Cs, ^{14}C	4/7	Pollen	Effective moisture	Tian et al. (2013)

(*continued on next page*)

Table 1 (*continued*)

Site no.	Site name	Lat. (°N)	Long. (°E)	Time period (cal BP)	Sample resolution (yr)[a]	Dating material	Dating method	No. of dates[b]	Proxies used[c]	Proxy indication	References
M38	Badain Jaran Desert	39.55	102.37	ca. 1200–0	6	–	Accumulative Chloride	–	Chloride concentrations in unsaturated zone	Groundwater recharge	Gates et al. (2008); Ma and Edmunds (2006)
M39	Eastern NW China (precipitation < 400 mm)	39.42	102.50	1420–0	10	–	History	–	Historical documents	Precipitation	Lee et al. (2015)
M40	Ulann Lake	44.51	103.65	ca. 17,000–0	50	Quartz	OSL	0/12	TOC, CN	Moisture	Lee et al. (2013)
M41	Gun Nuur	50.25	106.60	ca. 10,800–0	20	Bulk sediment, wood	^{14}C	5/48	Grain size, TOC, carbonate content, $\delta^{13}C_{org}$, diatom	Lake level (moisture)	Zhang et al. (2012)
M42	Kahf Defore	17.12	54.08	ca. 700–0	1	–	Annual growth band counting	–	Speleothem $\delta^{18}O$[e], speleothem annual band thickness	Precipitation	Fleitmann et al. (2004); Burns et al. (2002)
M43	NE Arabian Sea	24.83	65.92	ca. 4900–0	1	–	Varve counting	–	Varve thickness	Precipitation, river runoff	von Rad et al. (1999)
M44	Arabian Sea	21.80	68.00	ca. 1200–0	20	Planktonic foraminiferal	^{14}C	3/4	TOC, TN	Productivity (monsoon intensity, precipitation)	Agnihotri et al. (2002)
M45	Sahiya Cave	30.60	77.87	5760–0	1	–	^{230}Th	18/71	Speleothem $\delta^{18}O$	Precipitation	Kathayat et al. (2017)
M46	Western Himalaya	31.50	78.19	1030–0	1	–	Ring counting	–	Tree-ring width	Spring precipitation	Yadava et al. (2016)
M47	Dharamjali cave	29.52	80.21	ca. 1700–0	10	–	^{230}Th	2/5	Speleothem $\delta^{18}O$	Precipitation	Sanwal et al. (2013)
M48	Central and Northeastern India	18.90	81.90	ca. 1400–0	1	–	Annual growth band counting	–	Speleothem $\delta^{18}O$	Precipitation	Sinha et al. (2011)
M49	East Rongbuk	28.03	86.96	ca. 1000–0	6	–	Annual layer counting, ice flow model	–	Ice-core δD	Precipitation	Kaspari et al. (2007)
M50	Ngamring Tso	29.30	87.20	ca. 4100–0	30	Aquatic macrophyte, modern aquatic macrophyte, bulk organic matter	^{210}Pb, ^{137}Cs, ^{14}C	2/6	Grain size	Summer precipitation	Conroy et al. (2017)
M51	Linzhou County	30.30	91.50	870-(−50)	1	–	Ring counting	–	Tree-ring width	Precipitation	He et al. (2013b)
M52	Tiancai Lake	26.63	99.72	ca.12280–0	50	Plant remains, organic sediment	^{210}Pb, ^{137}Cs, ^{14}C	2/19	Pollen	Moisture	Xiao et al. (2014)
M53	Qinghai Lake	37.00	100.00	ca. 3500–0	15	Plant debris	^{14}C	0/2	%C37:4	Salinity (precipitation)	Liu et al. (2006)
M54	Lugu Lake	27.71	100.79	ca. 2900–0	25	Buried plant debris	^{137}Cs, ^{14}C	2/5	Grain size, C/N	Precipitation	Sheng et al. (2015)
M55	Ximencuo Lake	33.38	101.11	ca. 1000–0	15	Bulk organic carbon	^{210}Pb, ^{137}Cs	1	TOC, TN (total nitrogen)	Precipitation	Pu et al. (2013)
M56	Daotang Pond	36.96	101.25	ca. 1150–0	20	Organic bulk material	^{14}C	1/2	Pollen	Precipitation/moisture	Müller (2017)
M57	Shenqi Cave	28.93	103.10	2320–50	5	–	^{230}Th	20/35	Speleothem $\delta^{18}O$	Precipitation	Tan et al. (2018)
M58	Longxi Area	35.45	104.78	990-(−50)	10	–	History	–	Historical documents	Precipitation	Tan et al. (2008)
M59	Wanxiang Cave	33.32	105.00	ca. 1800–0	3	–	^{230}Th	11/19	Speleothem $\delta^{18}O$	Precipitation	Zhang et al. (2008)
M60	Huangye Cave	33.58	105.12	ca. 1800–0	5	–	Annual growth band counting, ^{230}Th	4/13	Speleothem $\delta^{18}O$	Precipitation	Tan et al. (2011)
M61	Zhijin Cave	26.66	105.68	ca. 1100–0	5	–	^{230}Th	4/5	Speleothem $\delta^{18}O$	Precipitation, summer/winter precipitaion ratio	Kuo et al. (2011)
M62	Eastern NW China (precipitation > 400 mm)	34.50	106.00	1420–0	10	–	History	–	Historical documents	Precipitation	Lee et al. (2015)
M63	Tianchi Lake	35.26	106.31	ca. 6200–0	5	*Abies* leaf macrofossils	^{14}C	2/17	Sediment redness	Precipitation	Zhou et al. (2010)
M64	Gouchi Lake	37.75	107.52	ca. 2400–0	25	Bulk sediment	^{14}C	3/9	Pollen	Moisture	Meng et al. (2009)
M65	Foyechi Pond	33.95	107.73	ca. 1000–0	40	–	^{14}C	2	Pollen	Precipitation	Tong et al. (1996)
M66	Furong Cave	29.23	107.90	ca. 2000–0	8	–	^{230}Th	2/5	Speleothem $\delta^{18}O$	Precipitation	Li et al. (2011b)

(*continued on next page*)

Table 1 (*continued*)

Site no.	Site name	Lat. (°N)	Long. (°E)	Time period (cal BP)	Sample resolution (yr)[a]	Dating material	Dating method	No. of dates[b]	Proxies used[c]	Proxy indication	References
M67	Foye Cave	33.67	109.08	ca. 1200–0	3	–	Annual growth band counting, ^{230}Th	1	Speleothem δ^{13}C	Moisture	Paulsen et al. (2003)
M68	Dajiuhu Peatland	31.48	110.06	ca. 2500–0	70	Peat, bulk sediment, wood	^{14}C	2/12	Pollen	Precipitation	He et al. (2003)
M69	Huguangyan Maar Lake	21.15	110.28	ca. 1300–0	5	Gyttja, leaf	^{137}Cs, ^{14}C	3	TOC, biogenic silica, TN	Precipitation	Chu et al. (2002)
M70	Heshang Cave	30.45	110.42	ca. 8800–0	100	–	Annual growth band counting, ^{230}Th	2/21	Speleothem delta δ^{18}O	Precipitation	Hu et al. (2008)
M71	Tengernur Lake	40.47	110.67	ca. 1700–0	40	–	OSL	1/2	Grain size, pollen	Moisture	Zhao et al. (2011)
M72	Gonghai Lake	38.90	112.23	ca. 1100–0	5	Terrestrial plant macrofossil	^{14}C	3/4	Magnetical parameters	Precipitation	Liu et al. (2011)
M73	Daihai Lake	40.55	112.66	ca. 10,300–0	35	Bulk sediment	^{14}C	0/8	Pollen	Precipitation	Xu et al. (2010)
M74	Cattle Pond	16.67	112.73	ca. 980–0	5	Plant caryopsis, TOC	^{210}Pb, ^{14}C	14/14	Grain size	Precipitation	Yan et al. (2011)
M75	North China	36.40	115.12	2000–0	10	–	History	–	Historical documents	Precipitation	Man (2009)
M76	Shihua Cave	39.83	115.67	ca. 2200–0	20	–	Annual growth band counting	–	Speleothem δ^{18}O , δ^{13}C	Precipitation	Hou et al. (2003)
M77	Longgan Lake	29.96	116.13	ca. 3000–0	35	–	^{14}C	–	Pollen	Precipitation	Tong et al. (1997)
M78	Dali Lake	43.26	116.60	ca. 12,000–0	10	Organic matter	^{14}C	4/18	TOC, TIC	Lake level (precipitation)	Xiao et al. (2008)
M79	Southern China	27.50	117.00	1450-(−50)	1	–	History	–	Historical documents	Precipitation	Zheng et al. (2006)
M80	Lower Huai River and Yangtz River Basin	32.36	117.84	1950–0	10	–	History	–	Historical documents	Precipitation	Man (2009)
M81	Jiufeng Mountain	26.87	118.72	ca. 1370–0	25	Humified Peat, wood	^{14}C	3/6	Cellulose δ^{13}C	Precipitation	Lei et al. (2017)
M82	Tsuifong Lake	24.50	121.60	ca. 1400–0	10	Plant fragment	^{210}Pb, ^{14}C	4/5	Diatom, $\delta^{15}N_{org}$, $\delta^{13}C_{org}$, magnetic susceptibility	pH, erosion (precipitation)	Wang et al. (2013c)
M83	Southern Okinawa Trough	24.80	122.49	ca. 1000–0	15	Planktonic foraminifera	^{14}C	5/6	Diatom	Salinity (precipitation)	Li et al. (2011c)
M84	Maili Pond	42.87	122.88	ca. 2000–0	25	Peat	^{14}C	2/6	Pollen	Precipitation	Ren, 1998
M85	Xiaolongwan Lake	42.30	126.35	ca. 1600–0	15	–	Varve counting	–	$\delta^{13}C_{org}$	Precipitation/moisture	Chu et al. (2009)
M86	Mulyoungari crater swamp	33.37	126.69	ca. 1100–80	20	Wood fragments, bulk sediments, plant remains	^{14}C	7/8	Pollen, diatom, δ^{13}C, C/N, TS (total sulfur)	Precipitation/moisture	Park et al. (2017)
M87	Korea	38.32	127.00	940-(−30)	10	–	History	–	Historical documents	Precipitation	Kim and Choi (1987)
C1	Tienshan Mountains	43.78	87.97	280-(−50)	1	–	Ring counting	–	Tree-ring width	Palmer drought severity index (moisture)	Li et al. (2006)
C2	Helan Mountains	38.90	106.03	160-(−50)	1	–	Ring counting	–	Tree-ring width	Palmer drought severity index (moisture)	Li et al. (2007)

The Holocene (H), last millennium (M), and past century (C) proxy records are numbered H1-H16, M1-M87 and C1-C2, respectively.

[a] Average resolution during the Holocene (sites H1-H16), the last millennium (sites M1-M87) or the past century (sites C1-C2). If there were multiple proxies for a site, the resolution was calculated using the most highly-resolved proxy.

[b] No. of dates within the Holocene (sites H1-H16), within the last millennium (sites M1-M87) or within the past century (sites C1-C2)/total dates in the sequence, ^{210}Pb/^{137}Cs/^{241}Am dates are counted as one.

[c] For the speleothem oxygen isotope records, only those validated by other independent precipitation records (instrumental or historical data) were used in our study.

[d] This means that the proxy indication is lake level and was further used to reflect river discharge variations in the original reference (similarly hereinafter).

[e] Discontinuous record.

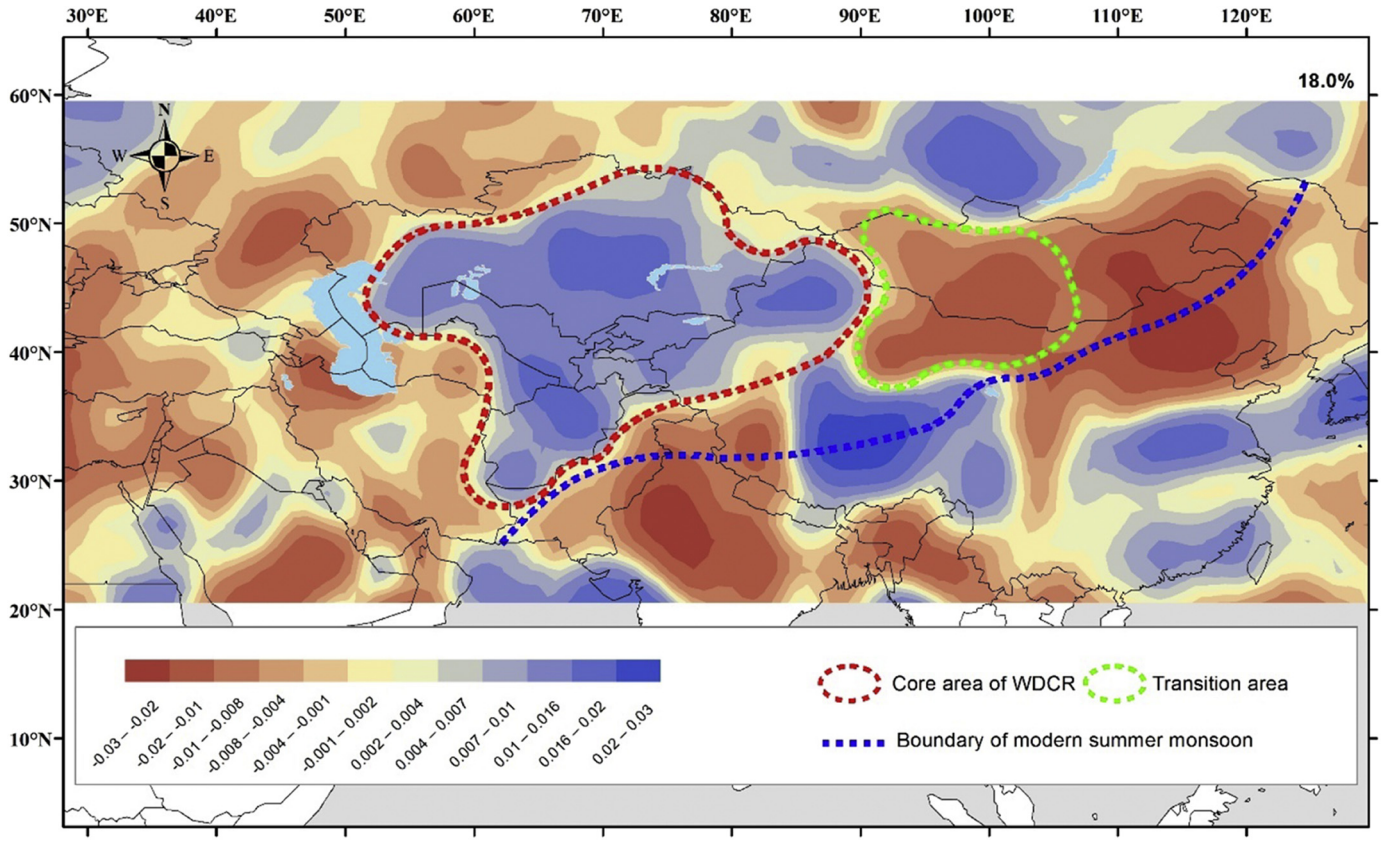

Fig. 2. EOF1 mode (18% total variance explained) computed from summer decadal precipitation during the period 1960–2010 (modified from Huang et al., 2015a). The area enclosed by the red dashed line is the core area of the 'westerlies-dominated climate regime' (WDCR), the area enclosed by the green dashed line is the transitional zone, and the blue dashed line shows the northern boundary of modern summer monsoon. (For interpretation of the references to colour in this figure legend, the reader is referred to the web version of this article.)

2016).

Based on knowledge of modern mid-latitude Asian climate changes, the core region of the WDCR (represented by the red dashed lines in Fig. 2) was used to improve our understanding of differences in moisture changes within arid central Asia during the Holocene. We used records of climatically-sensitive magnetic properties and soil colour of four well-dated loess-paleosol sequences from the northern slope of the Tienshan Mountains and the Yili River Valley, Xinjiang Province, to reconstruct the trends of regional moisture evolution (H5 in Fig. 1; Chen et al., 2016a). The results showed that the early Holocene mainly experienced a dry climate with loess accumulation; since ~6 ka, the climate gradually became wetter, resulting in the development of four paleosol layers, with strongest pedogenesis occurring in the late Holocene. In general, the moisture of the region increased gradually prior to 6 ka, and then rapidly, with the most humid period occurring during the late Holocene (Fig. 3a). The results of this study are consistent with other records from northern Xinjiang (Wang and Feng, 2013) and the Caspian Sea (H2 in Fig. 1; Leroy et al., 2014). Thus, we regard it as a representative pattern of Holocene climate change within the core area of the WDCR. The transitional belt between the core area of the WDCR and the monsoonal region (represented by the green dashed lines in Fig. 2), such as the mid-western Mongolian Plateau and the Gobi Desert of Inner Mongolia, are strongly influenced by the East Asian summer monsoon in addition to the westerlies, which explains why the pattern of moisture evolution of the entirety of arid central Asia (Chen et al., 2008, 2009b; Fig. 3b) differs somewhat from that of the core area.

The Holocene climatic evolution in the core area of the WDCR described above is also supported by climate model simulations (Chen et al., 2016a). These results demonstrate a trend of increasing summer and winter precipitation over the past 12,000 years, which was driven mainly by the enhanced westerlies. The detailed mechanism of this phenomenon is described in Section 6.

In contrast, the evolution of both the Indian summer monsoon (ISM) and the East Asian summer monsoon (EASM) exhibits different overall trends from moisture change in the core area of the WDCR during the Holocene. The following important points can be made. (1) Given an increasing dispute about the paleoclimatic significance of speleothem oxygen isotopes from Chinese caves (e.g. Dayem et al., 2010; Maher and Thompson, 2012; Tan, 2014; Liu et al., 2015; Baker et al., 2015; Chen et al., 2016b; Clemens et al., 2018), a new composite speleothem record from the Indian Subcontinent and Arabian Peninsula (Liu et al., 2019), where oxygen isotopes are an unambiguous precipitation proxy and where precipitation amount reflects ISM intensity (Neff et al., 2001; Sinha et al., 2015), was used to represent ISM variations. This record, together with other paleo-precipitation reconstructions (e.g. H15 in Fig. 1; Chen et al., 2014a), demonstrate that the ISM, driven primarily by changes in NHSI, gradually weakened during the Holocene (Fig. 3d). (2) The amount of precipitation in northern China is used to measure the EASM intensity (Chen et al., 2015a, 2016b). The pollen-based quantitative precipitation reconstruction from Gonghai Lake in northern China features a combination of both a robust chronology and an unambiguous proxy (H16 in Fig. 1; Chen et al., 2015a). This record, together with other paleo-precipitation reconstructions (e.g. Lu et al., 2013), indicates that the EASM intensity reached a maximum in the mid-Holocene, and its changes were controlled not only by NHSI but also by the westerlies circulation and Atlantic Meridional Overturning Circulation during the early Holocene, and by El Niño–Southern Oscillation (ENSO) during the late Holocene (Chen et al., 2015a; Fig. 3c). (3) In the transitional region between the monsoonal region and the

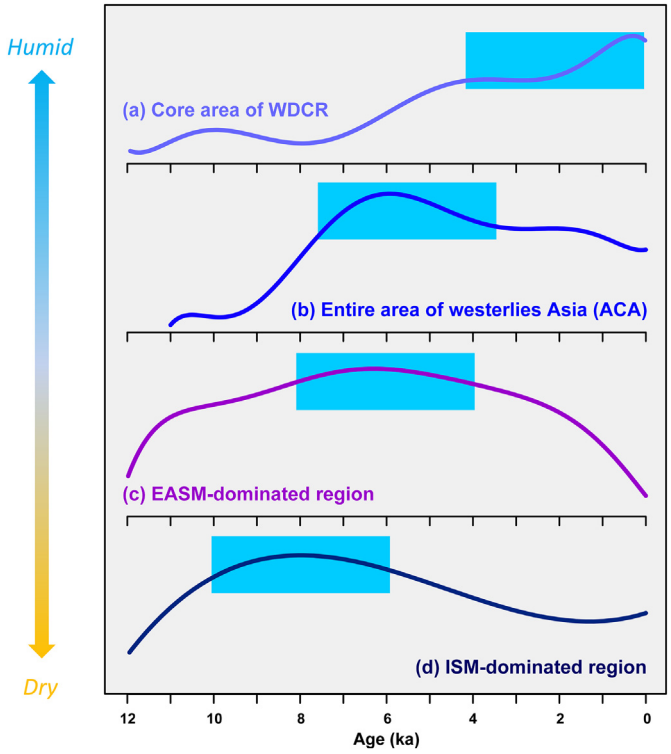

Fig. 3. Simplified moisture evolution patterns in different regions of Asia during the Holocene. (a) Core area of WDCR (according to the magnetic susceptibility record of the LJW10 section in Chen et al., 2016a), (b) the entire area of westerlies Asia (according to a synthesized regional moisture record in Chen et al., 2009a), (c) Eastern Asian Summer Monsoon (EASM)-dominated region (according to a precipitation reconstruction from Gonghai Lake in Chen et al., 2015a), and (d) Indian Summer Monsoon (ISM)-dominated region (according to a composite speleothem $\delta^{18}O$ record from the Indian Subcontinent and Arabian Peninsula in Liu et al., 2019).

core area of WDCR, the occurrence of a mid-Holocene moisture maximum may be primarily attributed to the advance of the EASM.

4. Spatial pattern of hydroclimatic changes on a centennial timescale during the last millennium

An investigation of the WDCR during the Holocene provides the framework for understanding the environmental evolution of arid central Asia. To further examine the paleoclimatic record of westerlies Asia on centennial timescales, we reconstructed high-resolution records of moisture variability from several key sites (e.g. M17 and M27 in Fig. 1) over the last millennium (Chen et al., 2006; Chen et al., 2009b), and focused on how regional moisture responded to temperature anomalies during the Medieval Warm Period (MWP; 1000–1300 CE) and the Little Ice Age (LIA; 1400–1900 CE) (IPCC, 2007). Five high-quality proxy records were then synthesized to evaluate the sequence of moisture changes in the Asian inland arid region (Chen et al., 2010). The results showed a dry climate during the MWP and a wet climate during the LIA, which may have been caused by north-south movements of the westerlies associated with the phase changes of the North Atlantic Oscillation (NAO).

To determine whether the WDCR during the Holocene on the sub-orbital timescale also exists on centennial timescales, 71 proxy records of precipitation/moisture with reliable chronologies spanning the past millennium from China and surrounding regions, were compiled to explore regional patterns of hydroclimatic variability (Chen et al., 2015b). In the present study, an updated dataset comprising 87 paleo-hydroclimatic records is used (M1-M87 in Fig. 1). The results (Fig. 4) indicated that the monsoonal region was generally wetter, whereas the arid region was generally drier, during the MWP compared to the LIA in mid-latitude Asia north of approx. 33°N. The anti-phased moisture variations in the two regions are roughly separated by the modern summer monsoon limit. Additionally, over the East Asian monsoon region (east of approx. 105°E), the northern part was generally wetter, whereas the southern part was generally drier during the MWP than during the LIA. The boundary of the two East Asia monsoon regions with opposite moisture variations, is around the Qinling Mountain Range - Huaihe River Valley. Therefore, the moisture contrast between westerlies Asia and mid-latitude monsoonal Asia existed not only on sub-orbital scales during the Holocene, but also on centennial scales during the last millennium. Combined with observational data, we suggest that ENSO could have been one of the dominant factors controlling hydrological and climatic changes in China and surroundings on centennial timescales. This hypothesis is supported by model simulations based on the Paleoclimate Modelling Intercomparison Project Phase III (PMIP3) (Shi et al., 2016). It should be noted that such relationships between ENSO and the spatial pattern of hydroclimatic variability for the last millennium were based mainly on statistical analysis, and the relevant dynamic processes are discussed in Section 6.

5. Pattern of precipitation/moisture changes on a decadal timescale over the past century

In comparison with that on centennial and longer timescales, climate change on decadal timescales is of more direct societal significance (e.g. Liang et al., 2006; Cook et al., 2010; Pederson et al., 2014). It has been demonstrated that the hydrothermal configuration of the Xinjiang region changed from 'warm and dry' to 'warm and wet' since the late 1980s (Shi et al., 2007). In addition, the area of terminal lakes in NW China has generally increased and many previously-desiccated lake basins have been refilled with water (Hu et al., 2002; Guo et al., 2003). Other studies have also identified increasing glacier ablation and stream runoff in inland river basins, such as those of the Tarim River, Shule River, Black River, and Shiyang River (Hao et al., 2008; Li et al., 2013; Gao et al., 2010; Chen et al., 2014b; e.g. Fig. 5d). All these phenomena are consistent with observed increasing precipitation and moisture in the region in the context of global warming (Ma and Fu, 2006; Feng et al., 2007; Qian and Qin, 2008; Jiang et al., 2009; Huang et al., 2013; e.g. Fig. 5b). Furthermore, values of the Palmer Drought Severity Index (PDSI) reconstructed by tree-ring records from the Tienshan Mountains suggest that soil moisture has generally increased over the past century in the Xinjiang region (C1 in Fig. 1; Li et al., 2006; Fig. 5a). For Central Asia, Chen et al. (2011) analyzed precipitation variability during the past 80 years and found an overall increasing trend despite some internal differences (Fig. 5c). These results all demonstrate that on the decadal scale precipitation, moisture, and stream runoff have gradually increased in the core area of the WDCR in the past century.

By contrast, the overall weakening trend of the Asian summer monsoon over the past century (Li and Zeng, 2003; Wang and Ding, 2006; Ding et al., 2008) resulted in decreased moisture (according to a tree-ring based PDSI reconstruction) across the monsoon fringes in the Helan Mountains (C2 in Fig. 1; Li et al., 2007; Fig. 5e). Observational data also indicate a substantial decrease in precipitation, and a strong drying trend in North China and the eastern part of NW China over the past five decades (Jin et al., 2005; Ma and Fu, 2006; Feng et al., 2007; Qian and Qin, 2008; Huang et al., 2016; Fig. 5f). Accordingly, the Haihe River and the Yellow River basins, located in North China, have experienced moderately increased evapotranspiration and substantially decreased river run-off (Bao et al., 2012; Zhang et al., 2016a; Fig. 5g).

Therefore, these results suggest that precipitation/moisture differences also existed between the core area of the WDCR and the eastern monsoonal region over the past century, and that the WDCR can be used to portray patterns of climatic change in mid-latitude Asia on decadal timescales. It was proposed that the location and strength of the

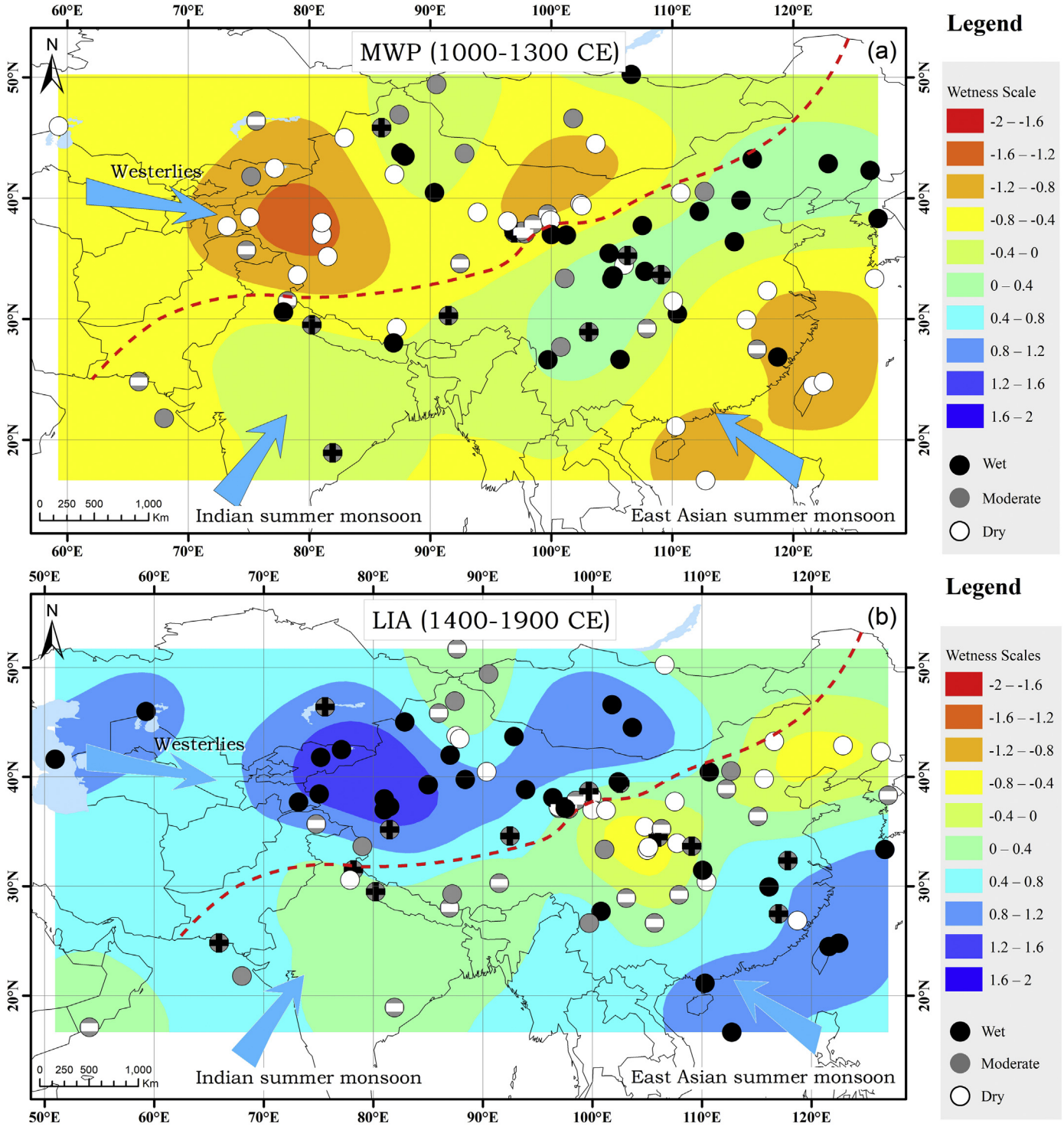

Fig. 4. Wetness map based on multi-proxy records during the MCA (a) and LIA (b) (updated and modified from Chen et al., 2015b). Wetness is classified into dry (scale = −2), moderate (scale = 0) and wet (scale = 2) categories. The 'moderately dry (scale = -1)' and 'moderately wet (scale = 1)' classes for the high-resolution records (with an average resolution better than 10 years) are indicated by '-' and '+' symbols overlain on grey solid circles, respectively. The colour map was generated by Kriging interpolation of wetness scales from individual sites.

westerlies may have played an important role in precipitation change in westerlies Asia in the past century (Rogers and Van, 1979; Aizen et al., 2001; Huang et al., 2013). On the other hand, ENSO could also have been one of the major factors influencing precipitation variations in monsoonal Asia during this period (Huang and Wu, 1989; Huang et al., 1999; Mathew et al., 2002; Feng and Hu, 2004; Huang et al., 2013). The interaction between the westerlies and ENSO, and the relative roles of the two factors in producing the WDCR on a decadal timescale, are discussed in Section 6.

6. Physical mechanisms of the westerlies-dominated climatic regime

We now investigate the physical mechanisms of the WDCR, with the

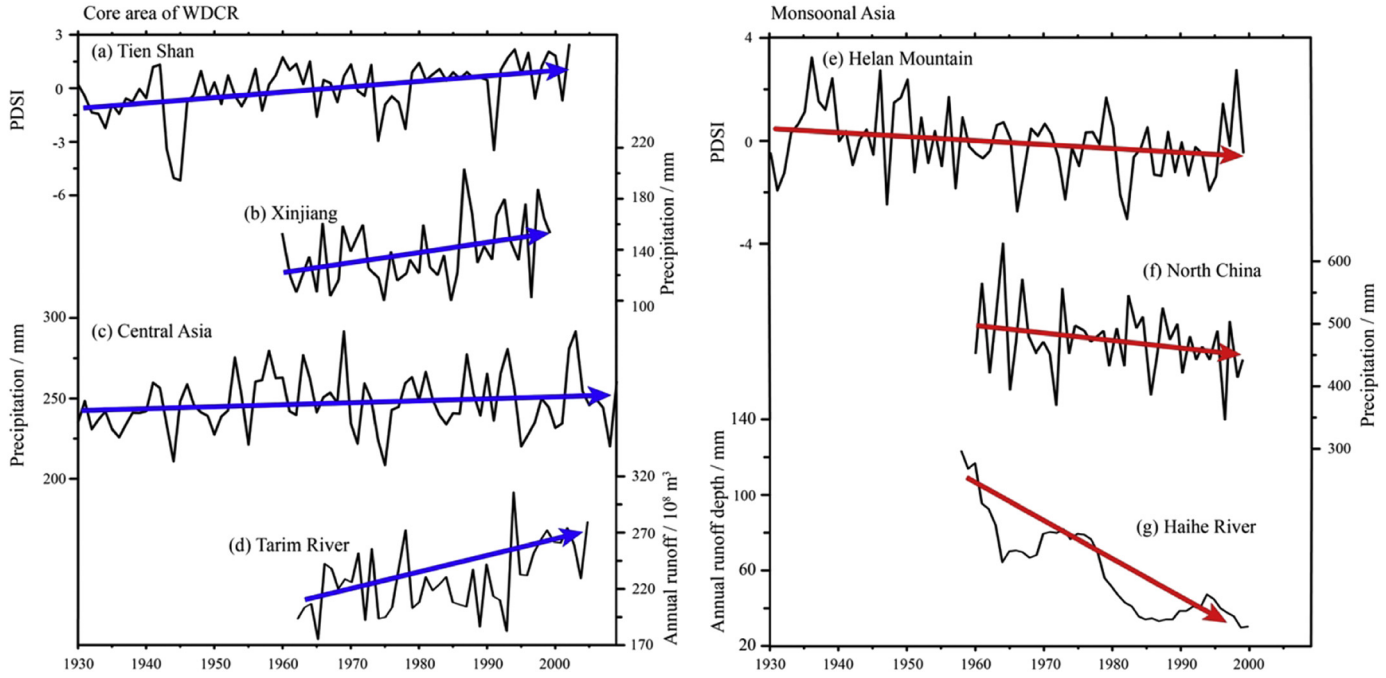

Fig. 5. Hydroclimatic changes in the core area of WDCR as indicated by the moisture patterns in Tienshan Mountains (a, after Li et al., 2006), annual precipitation in Xinjiang (b, after Qian and Qin, 2008) and Central Asia (d, after Chen et al., 2011), and annual runoff of the Tarim River (d, after Gao et al., 2010); and those in monsoonal Asia as indicated by the moisture patterns in Helan Mountain (e, after Li et al., 2007), annual precipitation in North China (f, after Qian and Qin, 2008) and annual runoff of the Haihe River (g, after Bao et al., 2012) during the past few decades. The arrows indicate the overall linear trend.

emphasis mainly on sub-orbital and centennial-to-decadal timescales.

On the sub-orbital scale, changes in incoming solar radiation (an external factor) have the dominant impact on the WDCR. Liu et al. (2009, 2014) performed a 21-kyr transient climate simulation experiment (TraCE-21 ka), considering both external and internal driving factors (including solar radiation, greenhouse gases, glacial melt water, and continental ice sheets). The results demonstrated that winter, summer, and annual precipitation all show an increasing trend in the core area of the WDCR since 12 ka (Chen et al., 2016a; Fig. 6b, c, d). A partial explanation is the weaker winter insolation during the early Holocene (Berger and Loutre, 1991; Fig. 6e), which resulted in decreased surface evaporation of water bodies (i.e., the Mediterranean Sea, Black Sea, and Caspian Sea) upwind of the core area of WDCR. At the same time, the weak winter insolation led to a smaller meridional radiation gradient between high- and mid-latitudes (Fig. 6f, g), which further decreased the intensity of the westerlies circulation (Jin et al., 2012). In summer, the relatively high temperature (Fig. 6h) caused by stronger insolation during the early Holocene led to a northward shift of the subtropical high, inhibiting precipitation in the core area of the WDCR. In addition, the stronger insolation accelerated the retreat of the Laurentide and Scandinavian Ice Sheets and increased meltwater discharge into the North Atlantic (Carlson and Clark, 2012), which also decreased its surface evaporation. By contrast, the increased winter insolation and decreased summer insolation during the late Holocene (Berger and Loutre, 1991) resulted in the reverse condition. Therefore, the increased precipitation/moisture since the early Holocene can be attributed to the combined effect of the increased evaporation of major water bodies upwind, the southward shift of the subtropical high, and the increased westerlies intensity in the mid-latitude region (Zhang et al., 2016b).

Overall, simulation results indicate an increasing trend in precipitation changes in the core area of the WDCR during the Holocene, which is consistent with our recent moisture reconstruction based on the loess-paleosol sequence (Chen et al., 2016a; Fig. 6a). The basic framework of the physical mechanisms that drive precipitation changes in this region during the early Holocene is summarized in Fig. 7.

Investigations of the driving mechanisms on centennial-decadal timescales suggest that the effects of internal factors (e.g. atmosphere-sea interaction) on the formation of the WDCR are more pronounced than those of external factors. On a decadal timescale, the 'Silk Road pattern (SRP)' (Enomoto et al., 2003), the regional manifestation of a circumglobal teleconnection (CGT; Ding and Wang, 2005; Chen and Huang, 2012) in Eurasia, is a key factor affecting precipitation changes in mid-latitude Asia. A negative SRP features negative height anomalies in Central Asia and positive height anomalies in the Mediterranean Sea and North China, leading to */strengthened (weakened) meridional winds in the core area of the WDCR (North China). This brings more (less) water vapor from the Indian Ocean and Arabian Sea, and subsequently increases (decreases) summer precipitation in the former (latter) region (Huang et al., 2015a, 2015b). In addition, recent studies indicated that latent heat anomalies in the Indian subcontinent influenced the location of the South Asian high, which affected the Indian monsoon intensity and subsequently caused an opposing pattern of precipitation changes between arid central Asia and mid-latitude monsoonal Asia (Wei et al., 2014, 2015).

The SRP is associated with both the Asian summer westerly jet stream and the Indian summer monsoon. On one hand, the enhancement of the jet stream serves as a wave guide that favors the transmission of a stationary Rossby wave and a zonal teleconnection (i.e. the SRP) (Enomoto et al., 2003; Chen and Huang, 2012). On the other hand, the CGT/SRP is believed to originate from the combined effects of downward airflow in the Mediterranean Sea and the heating of the Indian monsoon (Enomoto et al., 2003), with the latter surmised to have a greater effect (Ding and Wang, 2005; Ding et al., 2011). Furthermore, Ding and Wang (2005) found that the Indian summer monsoon plays a critical role in linking the CGT and ENSO.

Using simulations from the CESM-LME (Otto-Bliesner et al., 2016), we also analyzed the spatiotemporal variations of summer precipitation based on EOF analysis. The results suggest that a dry (wet) climate during the MWP (LIA) and a wet (dry) climate during the LIA (MWP) in westerlies Asia (mid-latitude monsoonal Asia), which is consistent with results from proxy records (Chen et al., 2015b). Based on the EOF

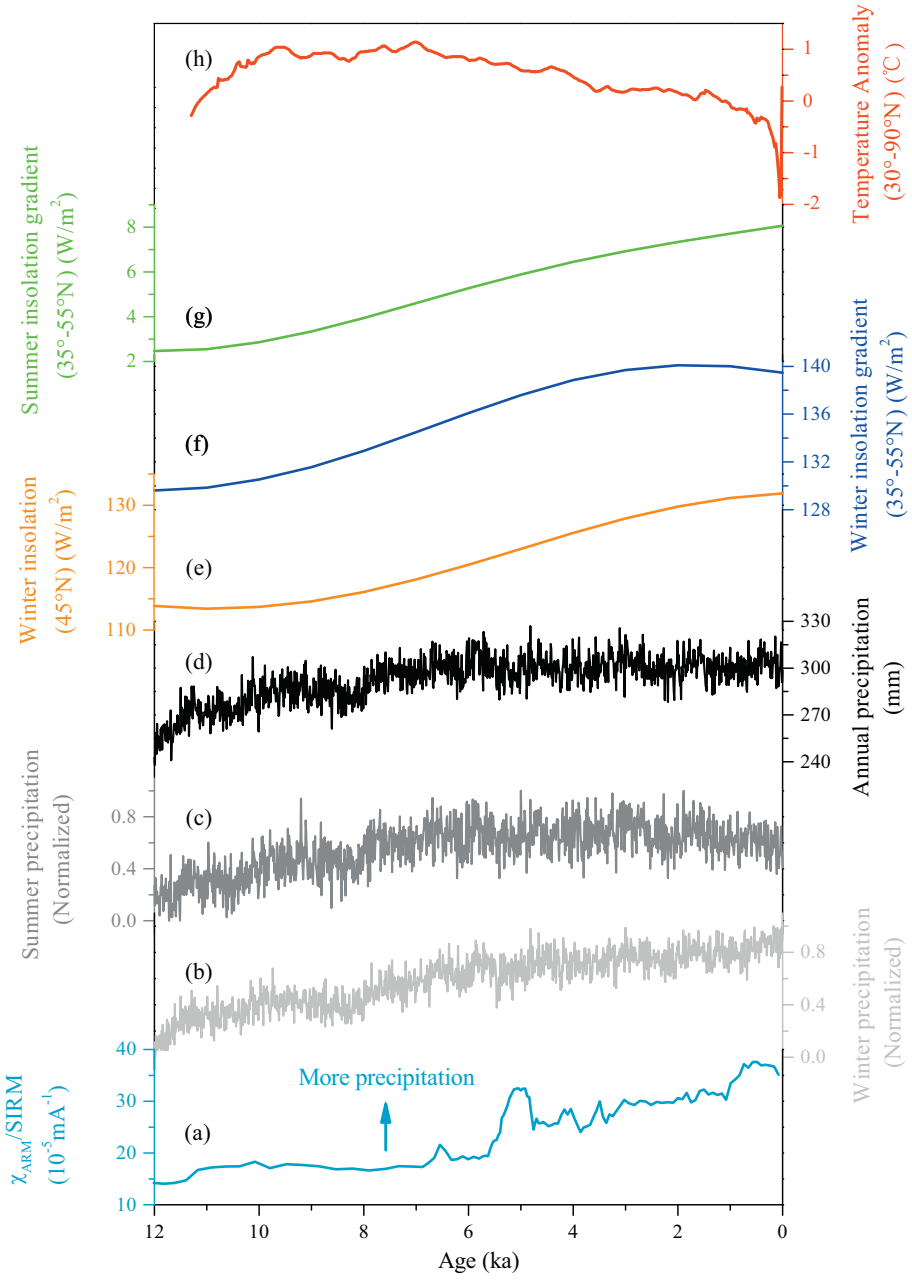

Fig. 6. Trends of precipitation/moisture evolution indicated by the χ_{ARM}/SIRM ratio of the LJW10 Holocene paleosol section (a, after Chen et al., 2016a); simulated regionally-averaged (35°-53°N, 60°-90°E) winter (b), summer (c) and annual (d) precipitation history for the core area of WDCR (after Chen et al., 2016a); winter insolation (e, after Berger and Loutre, 1991); strength of the westerlies in winter (f) and summer (g) represented by the insolation gradient between 35°N and 55°N (after Rossby, 1939); and Northern Hemisphere temperature (h, after Marcott et al., 2013).

results, a 'Silk Road pattern' index (SRPI) for the period of 850–2005 is defined, and the positive SRPI indicates northerly wind anomalies in the core area of the WDCR and positive SRP phases (Huang et al., 2015b, 2019). We found that positive and negative phases of the SRP dominated during the MWP and LIA, respectively (Fig. 8), which is consistent with the conditions on the decadal scale during the past century. It should be noted that this relationship based on the single model (e.g., CESM-LME) has some uncertainties, it will be very useful to perform similar analyses using other global climate models to check the robustness of our results. Furthermore, our results also support the argument developed using proxy records that ENSO could influence precipitation changes in westerlies Asia and monsoonal Asia on a centennial timescale (Chen et al., 2015b; Shi et al., 2016). This set of physical mechanisms can thus be applied to the formation of the WDCR on both the decadal and centennial timescales.

In summary, we suggest that the basic framework of the physical mechanisms generating the WDCR on decadal-centennial timescales has been convincingly established. Abnormal temperature changes in the Indian Ocean triggered divergent airflows in the upper level of the atmosphere, which then induced vorticity advection and influenced Rossby wave transmissions, resulting in the formation of a CGT/SRP in the subtropical region (Ding and Wang, 2005; Ding et al., 2011; Chen and Huang, 2012). In addition, Indian Ocean temperature anomalies also affect the location of the South Asian high, the intensity of the Indian monsoon (Wei et al., 2014, 2015), and the emergence of ENSO (Ding and Wang, 2005). Therefore, the SRP can be regarded as a link that connects the westerly jet stream, the South Asian high, the Indian monsoon, and ENSO, and provides a solid theoretical basis for

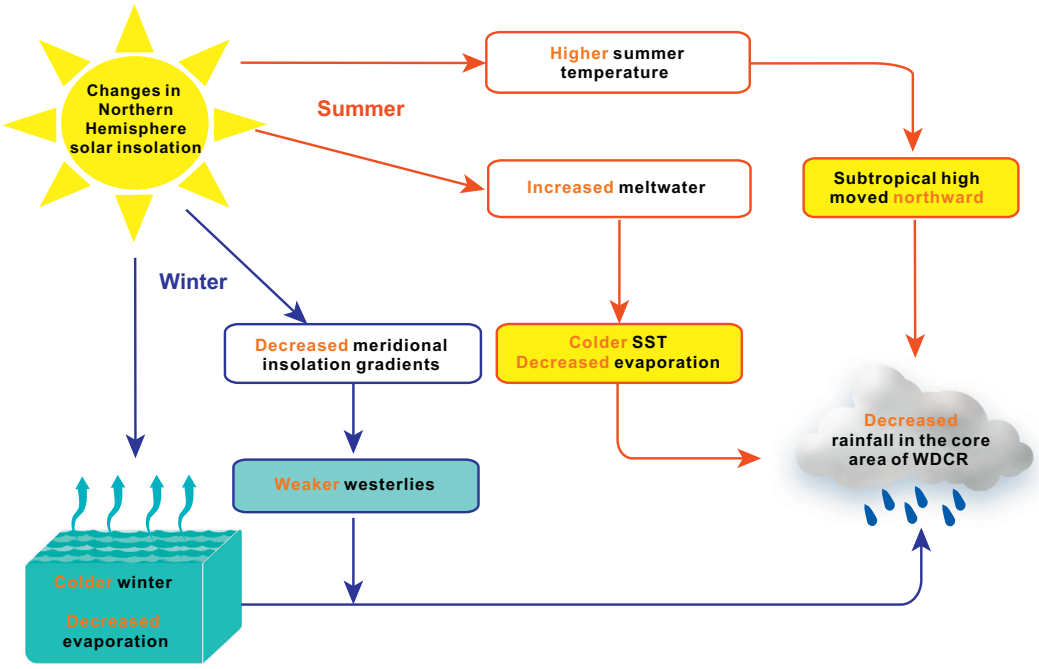

Fig. 7. Schematic diagram illustrating the physical mechanisms of the 'westerlies-dominated climate regime' during the early Holocene. The blue/red arrows denote the processes causing precipitation change in the core area of the WDCR in winter/summer, respectively. The conditions during the late Holocene are the opposite to this. (For interpretation of the references to colour in this figure legend, the reader is referred to the web version of this article.)

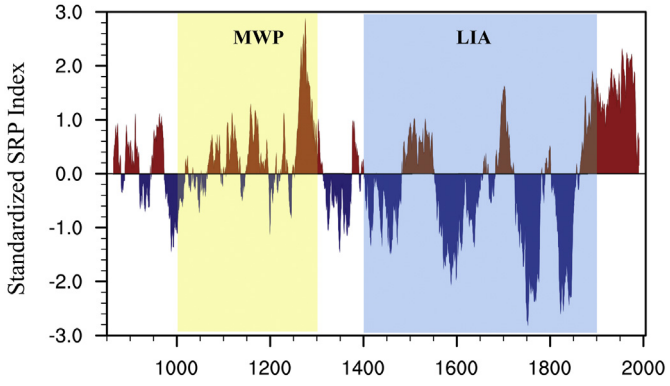

Fig. 8. The Silk Road pattern index from 850 to 2005 CE (modified from Huang et al., 2019). The yellow and blue vertical bands indicate the MWP and LIA, respectively. (For interpretation of the references to colour in this figure legend, the reader is referred to the web version of this article.)

explaining the formation of the WDCR (Fig. 9). Moreover, it is noteworthy that new simulation work is urgently needed to determine whether the mechanism on the decadal-centennial timescales is also applicable on sub-orbital or even longer timescales (e.g. Zhang and Jin, 2016). Last but not least, the relationships among the above-mentioned air-sea interactions may not always be stable, and are usually timescale-dependent. From a perspective of paleoclimate dynamics, such a question invariably remains challenging and requires persistent efforts.

7. Conclusions and future research questions

In this synthesis, we have integrated up-to-date paleo-moisture proxy records, observational data, and climate simulation results, pertaining to theories of the WDCR. We have demonstrated that precipitation/moisture differences existed between westerlies Asia and mid-latitude monsoonal Asia during the present Holocene interglacial period on sub-orbital, centennial, and decadal timescales. The core area of the WDCR is approximately equivalent to Central Asia and Xinjiang Province of China; its boundaries are the Caspian Sea (~50°E) to the west, the western end of the Hexi Corridor (~90°E) to the east, and the southern and northern limits of the Central Asian arid region to the south and north (~36–54°N). On a sub-orbital timescale, insolation-driven evaporation changes in major water bodies upwind, the northward-southward shift of the subtropical high, and the variation of westerlies intensity jointly control the WDCR; on centennial and decadal timescales, abnormal temperature changes within the Indian Ocean region that triggered the CGT/SRP, as well as changes in Asian summer westerly jet stream, South Asian high, Indian summer monsoon, and ENSO, are significant driving factors of the WDCR.

It is worth noting that given the difficulties in accurate pick-up of seasonal paleoclimate information, it is still hard to evaluate the uncertainties associated with the seasonality of proxy records in this study. Another issue lies in the fact that during the pre-industrial period, 'warm-dry'/'cold-wet' and 'warm-wet'/'cold-dry' shifts occurred in the core area of the WDCR and mid-latitude monsoon-dominated Asia, respectively. However, precipitation exhibits a rising (descending) trend in the former (the latter) region during the current warm period, demonstrating a 'warm-wet' ('warm-dry') configuration. This may potentially be attributed to the different impacts of natural and anthropogenic forcing on precipitation distribution (e.g. Liu et al., 2013) and need further investigation.

As studies of the WDCR become increasingly detailed, several new questions arise: (1) Are the moisture changes in westerlies Asia consistent with those of the monsoonal region on orbital timescales (e.g. recent several glacial-interglacial cycles), as suggested by a single loess-paleosol record from Tajikistan (Ding et al., 2002; Yang et al., 2006a)? (2) Do the asynchronous moisture changes between these two regions only exist on sub-orbital or shorter timescales during the interglacial periods rather than glacial periods, as indicated by the evidence presented herein for the Holocene, and by a recent study of aeolian deposits in the Tienshan Mountains for the last interglacial (Jia et al., 2018)? (3) What were the precipitation/moisture responses in westerlies Asia to abrupt temperature anomalies since the last glacial period (i.e. Dansgaard–Oeschger and Heinrich events and Bond cycles), and what are their phase relationships with those that have already been

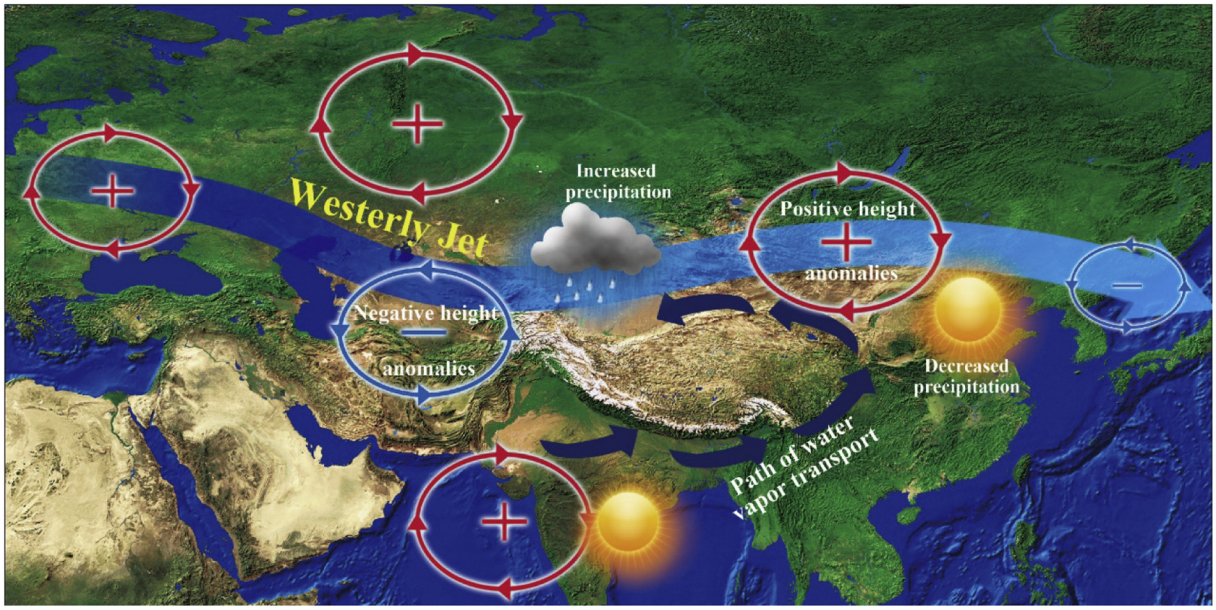

Fig. 9. Schematic diagram illustrating the physical mechanisms of the 'westerlies-dominated climate regime' on decadal-centennial timescales (modified from Huang et al., 2015a). Clouds and sun indicate more and less precipitation, respectively. The arrows denote water vapor transport paths, and the circles represent upper level geopotential height anomalies.

identified in mid-latitude monsoonal Asia? (4) As global warming continues, will the westerlies Asia become wetter or drier? And will the WDCR still exist given likely future moisture changes within mid-latitude monsoonal Asia? We hope that the results of the present study can serve as a foundation for addressing these questions as well as facilitate the formulation of theories regarding environmental changes in arid regions, and provide a scientific basis for arid region remediation and ecological restoration programs in response to future global changes.

Acknowledgements

This research was funded by the National Key R&D Program of China (Grant No. 2018YFA0606404), the National Natural Science Foundation of China (Grant Nos. 41822102 and 41877446), the International Partnership Program of Chinese Academy of Sciences (Grant No. 131C11KYSB20160061), and the National Social Science Foundation of China (Grant No. 18ZDA172). We thank Dr. Jan Bloemendal for considerably improving the English language.

References

Agnihotri, R., Dutta, K., Bhushan, R., Somayajulu, B.L.K., 2002. Evidence for solar forcing on the Indian monsoon during the last millennium. Earth Planet. Sci. Lett. 198, 521–527.
Aichner, B., Feakins, S.J., Lee, J.E., Herzschuh, U., Liu, X., 2015. High-resolution leaf wax carbon and hydrogen isotopic record of the late Holocene paleoclimate in arid Central Asia. Clim. Past 11, 619–633.
Aizen, E.M., Aizen, V.B., Melack, J.M., Nakamura, T., Ohta, T., 2001. Precipitation and atmospheric circulation patterns at midlatitudes of Asia. Int. J. Climatol. 21, 535–556.
An, Z., Colman, S.M., Zhou, W., Li, X., Brown, E.T., Jull, A.J.T., Cai, Y., Huang, Y., Lu, X., Chang, H., Song, Y., Sun, Y., Xu, H., Liu, W., Jin, Z., Liu, X., Cheng, P., Liu, Y., Ai, L., Li, X., Liu, X., Yan, L., Shi, Z., Wang, X., Wu, F., Qiang, X., Dong, J., Lu, F., Xu, X., 2012. Interplay between the Westerlies and Asian monsoon recorded in Lake Qinghai sediments since 32 ka. Sci. Rep. 2, 619.
An, C.B., Tao, S.C., Zhao, J., Chen, F.H., Lv, Y.B., Dong, W.M., Li, H., Zhao, Y.T., Jin, M., Wang, Z., 2013. Late Quaternary (30.7–9.0 cal ka BP) vegetation history in Central Asia inferred from pollen records of Lake Balikun, Northwest China. J. Paleolimnol. 49, 145–154.
Anderson, D.M., Overpeck, J.T., Gupta, A.K., 2002. Increase in the Asian southwest monsoon during the past four centuries. Science 297, 596–599.
Baker, A.J., Sodemann, H., Baldini, J.U., Breitenbach, S.F., Johnson, K.R., Hunen, J., Zhang, P., 2015. Seasonality of westerly moisture transport in the East Asian summer monsoon and its implications for interpreting precipitation $\delta^{18}O$. J. Geophys. Res. Atmos. 120, 5850–5862.
Bao, Z.X., Zhang, J.Y., Wang, G.Q., Fu, G.B., He, R.M., Yan, X.L., Jin, J.L., Liu, Y.L., Zhang, A.J., 2012. Attribution for decreasing streamflow of the Haihe River basin, northern China: climate variability or human activities? J. Hydrol. 460, 117–129.
Berger, A., Loutre, M.F., 1991. Insolation values for the climate of the last 10 million years. Quat. Sci. Rev. 10, 297–317.
Boomer, I., Aladin, H., Plotnikov, I., Whatley, R., 2000. The palaeolimnology of the Aral Sea: a review. Quat. Sci. Rev. 19, 1259–1278.
Burns, S.J., Fleitmann, D., Mudelsee, M., Neff, U., Matter, A., Mangini, A., 2002. A 780-year annually resolved record of Indian Ocean monsoon precipitation from a speleothem from South Oman. J. Geophys. Res. 107. https://doi.org/10.1029/2001JD001281.
Cai, Y., Chiang, J.C.H., Breitenbach, S.F.M., Tan, L., Cheng, H., Edwards, R.L., An, Z., 2017. Holocene moisture changes in western China, Central Asia, inferred from stalagmites. Quat. Sci. Rev. 158, 15–28.
Carlson, A.E., Clark, P.U., 2012. Ice sheet sources of sea level rise and freshwater discharge during the last deglaciation. Rev. Geophys. 50https://doi.org/10.1029/2011RG000371. RG4007.
Chen, G.S., Huang, R.H., 2012. Excitation mechanisms of the teleconnection patterns affecting the July precipitation in Northwest China. J. Clim. 25, 7834–7851.
Chen, F.H., Wu, W., Holmes, J.A., Madsen, D.B., Zhu, Y., Jin, M., Oviatt, C.G., 2003. A mid-Holocene drought interval as evidenced by lake desiccation in the Alashan Plateau, Inner Mongolia. Chin. Sci. Bull 48, 1401–1410.
Chen, F.H., Huang, X.Z., Zhang, J.W., Holmes, J.A., Chen, J.H., 2006. Humid little ice age in arid Central Asia documented by Bosten Lake, Xinjiang, China. Sci. China Earth Sci. 49, 1280–1290.
Chen, F.H., Yu, Z.C., Yang, M.L., Ito, E., Wang, S.M., David, B.M., Huang, X.Z., Zhao, Y., Sato, T., Birks, H.J.B., Boomer, I., Chen, J.H., An, C.B., Wünnemann, B., 2008. Holocene moisture evolution in arid Central Asia and its out-of-phase relationship with Asian monsoon history. Quat. Sci. Rev. 27, 351–364.
Chen, F.H., Chen, J.H., Huang, W., 2009a. A discussion on the westerly-dominated climate model in mid-latitude Asia during the modern interglacial period. Earth Sci. Front. 16, 23–32 (in Chinese with English abstract).
Chen, J.H., Chen, F.H., Zhang, E.L., Brooks, S.J., Zhang, A.F., Zhang, J.W., 2009b. A 1000-year chironomid-based salinity reconstruction from varved sediments of Sugan Lake, Qaidam Basin, arid Northwest China, and its palaeoclimatic significance. Chin. Sci. Bull. 54, 3749–3759.
Chen, F.H., Chen, J.H., Holmes, J., Boomer, I., Austin, P., Gates, J.B., Wang, N.L., Brooks, S.J., Zhang, J.W., 2010. Moisture changes over the last millennium in arid Central Asia: a review, synthesis and comparison with monsoon region. Quat. Sci. Rev. 29, 1055–1068.
Chen, F.H., Huang, W., Jin, L.Y., Chen, J.H., Wang, J.S., 2011. Spatiotemporal precipitation variations in the arid Central Asia in the context of global warming. Sci. China Earth Sci. 54, 1812–1821.
Chen, F.H., Chen, X.M., Chen, J.H., Zhou, A.F., Wu, D., Tang, L.Y., Zhang, X.J., Huang, X.Z., Yu, J.Q., 2014a. Holocene vegetation history, precipitation changes and Indian summer monsoon evolution documented from sediments of Xingyun Lake, south-West China. J. Quat. Sci. 29, 661–674.
Chen, Y.N., Li, Z., Fan, Y.T., Wang, H.J., Fang, G.H., 2014b. Research progress on the impact of climate change on water resources in the arid region of Northwest China. Acta Geograph. Sin. 69, 1295–1304 (in Chinese with English abstract).
Chen, F.H., Xu, Q.H., Chen, J.H., Birks, H.J.B., Liu, J.B., Zhang, S.R., Jin, L.Y., An, C.B.,

Telford, R.J., Cao, X.Y., Wang, Z.L., Zahng, X.J., Selvaraj, K., Lü, H.Y., Li, Y.C., Zheng, Z., Wang, H.P., Zhou, A.F., Dong, G.H., Zhang, J.W., Huang, X.Z., Bloemendal, J., Rao, Z.G., 2015a. East Asian summer monsoon precipitation variability since the last deglaciation. .. Sci. Rep. 5, 11186.
Chen, J.H., Chen, F.H., Feng, S., Huang, W., Liu, J.B., Zhou, A.F., 2015b. Hydroclimatic changes in China and surroundings during the medieval climate Anomaly and Little Ice Age: spatial patterns and possible mechanisms. Quat. Sci. Rev. 107, 98–111.
Chen, F.H., Jia, J., Chen, J.H., Li, G.Q., Zhang, X.J., Xie, H.C., Xia, D.S., Huang, W., An, C.B., 2016a. A persistent Holocene wetting trend in arid Central Asia, with wettest conditions in the late Holocene, revealed by multi-proxy analyses of loess-paleosol sequences in Xinjiang, China. Quat. Sci. Rev. 146, 134–146.
Chen, J.H., Rao, Z.G., Liu, J.B., Huang, W., Feng, S., Dong, G.H., Hu, Y., Xu, Q.H., Chen, F.H., 2016b. On the timing of the East Asian summer monsoon maximum during the Holocene—does the speleothem oxygen isotope record reflect monsoon rainfall variability? Sci. China Earth Sci. 59, 2328–2338.
Chen, J., Huang, W., Jin, L.Y., Chen, J.H., Chen, S.Q., Chen, F.H., 2018. A climatological northern boundary index for the East Asian summer monsoon and its interannual variability. Sci. China Earth Sci. 61, 13–22.
Cheng, H., Spötl, C., Breitenbach, S.F.M., Sinha, A., Wassenburg, J.A., Jochum, K.P., Scholz, D., Li, X., Yi, L., Peng, Y., Lv, Y., Zhang, P., Votintseva, A., Loginov, V., Ning, Y., Kathayat, G., Edwards, R.L., 2016. Climate variations of Central Asia on orbital to millennial timescales. Sci. Rep. 6, 36975.
Chu, G.Q., Liu, J.Q., Sun, Q., Lu, H.Y., Gu, Z.Y., Wang, W.Y., Liu, T.S., 2002. The 'Mediaeval warm period' drought recorded in Lake Huguangyan, tropical South China. The Holocene 12, 511–516.
Chu, G., Sun, Q., Wang, X., Li, D., Rioual, P., Qiang, L., Han, J., Liu, J., 2009. A 1600 year multiproxy record of paleoclimatic change from varved sediments in Lake Xiaolongwan, northeastern China. J. Geophys. Res. 114https://doi.org/10.1029/2009jd012077. D22108.
Clark, P.U., Dyke, A.S., Shakun, J.D., Carlson, A.E., Clark, J., Wohlfarth, B., Mitrovica, J.X., Hostetler, S.W., McCabe, A.M., 2009. The last glacial maximum. Science 325, 710–714.
Clemens, S.C., Holbourn, A., Kubota, Y., Lee, K.E., Liu, Z., Chen, G., Nelson, A., Fox-Kemper, B., 2018. Precession-band variance missing from East Asian monsoon runoff. Nat. Commun. 9, 3364.
Conroy, J.L., Hudson, A.M., Overpeck, J.T., Liu, K.B., Wang, L., Cole, J.E., 2017. The primacy of multidecadal to centennial variability over late-Holocene forced change of the Asian Monsoon on the southern Tibetan Plateau. Earth Planet. Sci. Lett. 458, 337–348.
Cook, E.R., Anchukaitis, K.J., Buckley, B.M., D'Arrigo, R.D., Jacoby, G.C., Wright, W.E., 2010. Asian monsoon failure and megadrought during the last millennium. Science 328, 486–489.
Cui, L.L., Wang, X., Shen, J., Ding, Z.L., 2015. Changes in distribution and compound-specific carbon isotope compositions of n-alkanes as recorded in Lugu Lake sediments from southwestern China since last Glacial Maximum and implications for paleovegetation evolution. Quat. Sci. 35, 871–880 (in Chinese with English abstract).
Dayem, K.E., Molnar, P., Battisti, D.S., Roe, G.H., 2010. Lessons learned from oxygen isotopes in modern precipitation applied to interpretation of speleothem records of paleoclimate from eastern Asia. Earth Planet. Sci. Lett. 295, 219–230.
Ding, Q.H., Wang, B., 2005. Circumglobal teleconnection in the Northern Hemisphere summer. J. Clim. 18, 3483–3505.
Ding, Z.L., Ranov, V., Yang, S.L., Finaev, A., Han, J.M., Wang, G.A., 2002. The loess record in southern Tajikistan and correlation with Chinese loess. Earth Planet. Sci. Lett. 200, 387–400.
Ding, Y.H., Wang, Z.Y., Sun, Y., 2008. Inter-decadal variation of the summer precipitation in East China and its association with decreasing Asian summer monsoon. Part I: Observed evidences. Int. J. Climatol. 28, 1139–1161.
Ding, Q.H., Wang, B., Wallace, J.M., Branstator, G., 2011. Tropical-extratropical teleconnections in boreal summer: Observed interannual variability. J. Clim. 24, 1878–1896.
Dorofeyuk, N.I., Tarasov, P.E., 1998. Vegetation and lake levels in Northern Mongolia in the last 12,500 years as indicated by data of pollen and diatom analyses. Stratigr. Geol. Correl. 6, 70–83.
Enomoto, T., Hoskins, B.J., Matsuda, Y., 2003. The formation mechanism of the Bonin high in August. Q. J. R. Meteorol. Soc. 129, 157–178.
Feng, S., Fu, Q., 2013. Expansion of global drylands under a warming climate. Atmos. Chem. Phys. 13, 10081–10094.
Feng, S., Hu, Q., 2004. Variations in the teleconnection of ENSO and summer rainfall in Northern China: a role of the Indian summer monsoon. J. Clim. 17, 4871–4881.
Feng, Z.D., Wang, W.G., Guo, L.L., Khosbayar, P., Narantsetseg, T., Jull, A.J.T., An, C.B., Li, X.Q., Zhang, H.C., Ma, Y.Z., 2005. Lacustrine and eolian records of Holocene climate changes in the Mongolian Plateau: preliminary results. Quat. Int. 136, 25–32.
Feng, Z.D., An, C.B., Wang, H.B., 2006. Holocene climatic and environmental changes in the arid and semi-arid areas of China: a review. The Holocene 16, 119–130.
Feng, S., Nadarajah, S., Hu, Q., 2007. Modeling annual extreme precipitation in China using generalized extreme value distribution. J. Meteorol. Soc. Jpn. 85, 599–613.
Feng, Z.D., Wu, H.N., Zhang, C.J., Ran, M., Sun, A.Z., 2013. Bioclimatic change of the past 2500 years within the Balkhash Basin, eastern Kazakhstan, Central Asia. Quat. Int. 311, 63–70.
Ferronskii, V.I., Polyakov, V.A., Brezgunov, V.S., Vlasova, L.S., Karpychev, Y.A., Bobkov, A.F., Romaniovskii, V.V., Johnson, T., Richetts, D., Rasmssen, K., 2003. Variations in the hydrological regime of Kara-Bogaz-Gol Gulf, Lake Issyk-Kul, and the Aral Sea assessed based on data of bottom sediment studies. Water Resour. 30, 252–259.
Fleitmann, D., Burns, S.J., Neff, U., Mudelsee, M., Mangini, A., Matter, A., 2004. Palaeoclimatic interpretation of high-resolution oxygen isotope profiles derived from annually laminated speleothems from Southern Oman. Quat. Sci. Rev. 23, 935–945.
Fleitmann, D., Burns, S.J., Mangini, A., Mudelsee, M., Kramers, J., Villa, I., Neff, U., Al-Subbary, A.A., Buettner, A., Hippler, D., Matter, A., 2007. Holocene ITCZ and Indian monsoon dynamics recorded in stalagmites from Oman and Yemen (Socotra). Quat. Sci. Rev. 26, 170–188.
Fontes, J.-C., Gasse, F., Gibert, E., 1996. Holocene environmental changes in Lake Bangong basin (Western Tibet). Part 1: chronology and stable isotopes of carbonates of a Holocene lacustrine core. Palaeogeogr. Palaeoclimatol. Palaeoecol. 120, 25–47.
Fowell, S.J., Hansen, B.C.S., Peck, J.A., Khosbayer, P., Ganbold, E., 2003. Mid to late Holocene climate evolution of the Lake Telmen Basin, North Central Mongolia, based on palynological data. Quat. Res. 59, 353–363.
Gao, X., Ye, B.S., Zhang, S.Q., Qiao, C.J., Zhang, X.W., 2010. Sci. China Earth Sci. 53, 880–891 Glacier runoff variation and its influence on river runoff during 1961-2006 in the Tarim River Basin, China.
Gates, J.B., Edmunds, W.M., Ma, J.Z., Sheppard, P.R., 2008. A 700-year history of groundwater recharge in the drylands of NW China. The Holocene 18, 1045–1054.
Grunert, J., Lehmkuhl, F., Michael, W., 2000. Paleochimatic evolution of the Uvs Nuur basin and adjacent areas (Western Mongolia). Quat. Int. 65, 171–192.
Guo, N., Zhang, J., Liang, Y., 2003. Climate change indicated by the recent change of inland lakes in Northwest China. J. Glaciol. Geocryol. 25, 211–214 (in Chinese with English abstract).
Han, S.T., Qu, Z., 1992. Inland Holocene climatic features recorded in Balikun lake, northern Xinjiang. Sci. China Ser. B 11, 1201–1209 (in Chinese).
Han, S.T., Wu, N.Q., Li, Z.Z., 1993. Inland climate changes in Dzungaria during the late Pleistocene Epoch. Geogr. Res. 12, 47–54 (in Chinese with English abstract).
Hao, X.M., Chen, Y.N., Xu, C.C., Li, W.H., 2008. Impacts of climate change and human activities on the surface runoff in the Tarim River Basin over the last fifty years. Water Resour. Manag. 22, 1159–1171.
He, B.Y., Zhang, S., Cai, S.M., 2003. Climatic changes recorded in peat from the Dajiu Lake basin in Shennongjia since the last 2600 years. Mar. Geol. Quat. Geol. 23, 109–115 (in Chinese with English abstract).
He, Y., Zhao, C., Wang, Z., Wang, H., Song, M., Liu, W., Liu, Z., 2013a. Late Holocene coupled moisture and temperature changes on the northern Tibetan Plateau. Quat. Sci. Rev. 80, 47–57.
He, M., Yang, B., Bräuning, A., Wang, J., Wang, Z., 2013b. Tree-ring derived millennial precipitation record for the south-central Tibetan Plateau and its possible driving mechanism. The Holocene 23, 36–45.
Herzschuh, U., 2006. Palaeo-moisture evolution in monsoonal Central Asia during the last 50,000 years. Quat. Sci. Rev. 25, 163–178.
Herzschuh, U., Tarasov, P., Wünnemann, B., Hartmann, K., 2004. Holocene vegetation and climate of the Alashan Plateau, NW China, reconstructed from pollen data. Palaeogeogr. Palaeoclimatol. Palaeoecol. 211, 1–17.
Holmes, J.A., Cook, E.R., Yang, B., 2009. Climate change over the past 2000 years in Western China. Quat. Int. 194, 91–107.
Hong, B., Gasse, F., Uchida, M., Hong, Y., Leng, X., Shibata, Y., An, N., Zhu, Y., Wang, Y., 2014. Increasing summer rainfall in arid eastern-Central Asia over the past 8500 years. Sci. Rep. 4, 5279.
Hou, J.Z., Tan, M., Cheng, H., Liu, T.S., 2003. Stable isotope records of plant cover change and monsoon variation in the past 2200 years: evidence from laminated stalagmites in Beijing, China. Boreas 32, 304–313.
Hu, R.J., Jiang, F.Q., Wang, Y.J., Fan, Z.L., 2002. A study on signals and effects of climatic pattern change from warm-dry to warm-wet in Xinjiang. Arid Land Geo. 25, 194–200 (in Chinese with English abstract).
Hu, C.Y., Henderson, G.M., Huang, J.H., Xie, S., Sun, Y., Johnson, K.R., 2008. Quantification of Holocene Asian monsoon rainfall from spatially separated cave records. Earth Planet. Sci. Lett. 266, 221–232.
Huang, X.Z., 2006. Holocene Climate Variability of Arid Central Asia Documented by Bosten Lake, Xinjiang, China. Ph.D. Dissertation. Lanzhou University (in Chinese with English abstract).
Huang, R.H., Wu, Y.F., 1989. The influence of ENSO on the summer climate change in China and its mechanism. Adv. Atmos. Sci. 6, 21–32.
Huang, R.H., Xu, Y.H., Zhou, L.T., 1999. The interdecadal variation of summer precipitations in China and the drought trend in North China. Plat. Meteorol. 18, 465–476 (in Chinese with English abstract).
Huang, X.Z., Chen, F.H., Fan, Y.X., Yang, M.L., 2009. Dry late-glacial and early Holocene climate in arid Central Asia indicated by lithological and palynological evidence from Bosten Lake. China. Quat. Int. 194, 19–27.
Huang, W., Chen, F.H., Feng, S., Chen, J.H., Zhang, X.J., 2013. Interannual precipitation variations in the midlatitude Asia and their association with large scale atmospheric circulation. Chin. Sci. Bull. 58, 3963–3968.
Huang, W., Chen, J.H., Zhang, X.J., Feng, S., Chen, F.H., 2015a. Definition of the core zone of the "westerlies-dominated climatic regime", and its controlling factors during the instrumental period. Sci. China Earth Sci. 58, 676–684.
Huang, W., Feng, S., Chen, J.H., Chen, F.H., 2015b. Physical mechanisms of the summer precipitation variations in the Tarim Basin, Northwestern China. J. Clim. 28, 3579–3591.
Huang, J.P., Yu, H.P., Guan, X.D., Wang, G.Y., Guo, R.X., 2016. Accelerated dryland expansion under climate change. Nat. Clim. Chang. 6, 166–171.
Huang, W., Feng, S., Liu, C., Chen, J., Chen, J.H., Chen, F.H., 2018. Changes of climate regimes during the last millennium and the twenty-first century simulated by the Community Earth System Model. Quat. Sci. Rev. 180, 42–56.
Huang, W., Feng, S., Chen, J.H., Zhang, X., Liu, C., Chen, F.H., 2019. Physical Mechanisms of the Westerlies-Dominated Climatic Regime (WDCR) during the Last Millennium. (in preparation).
IPCC, Solomon, S., Qin, D., Manning, M., Chen, Z., Marquis, M., Averyt, K.B., Tignor, M., Miller, H.L., 2007. Climate change 2007: the physical science basis. In: Contribution of Working Group I to the Fourth Assessment Report of the Intergovernmental Panel

on Climate Change. Cambridge University Press, Cambridge, United Kingdom and New York.
Jia, J., Gao, F.Y., Xia, D.S., Huang, W., Chen, F.H., 2018. Moisture variations in arid Central Asia and its out-of-phase relationship with the Asian Monsoon during MIS 5: evidence from loess records. J. Quat. Sci. https://doi.org/10.1002/jqs.3024.
Jiang, Q.F., Shen, J., Liu, X.Q., Zhang, E.L., Xiao, X.Y., 2007. A high resolution climatic change since Holocene inferred from multi-proxy of lake sediment in westerly area of China. Chin. Sci. Bull. 52, 1970–1979.
Jiang, D.B., Su, M.F., Wei, R.Q., Liu, B., 2009. Variation and projection of drought and wet conditions in Xinjiang. Chin. J. Atmos. Sci. 33, 90–98 (in Chinese with English abstract).
Jiang, Q.F., Shen, J., Liu, X.Q., Ji, J.F., 2010. Environmental changes recorded by Lake sediments from Lake Jili, Xinjiang during the past 2500 years. J. Lake Sci. 22, 119–126 (in Chinese with English abstract).
Jin, L.Y., Fu, J.L., Chen, F.H., 2005. Spatial differences of precipitation over Northwest China during the last 44 years and its response to global warming. Sci. Geogr. Sin. 25, 567–572 (in Chinese with English abstract).
Jin, L.Y., Chen, F.H., Morrill, C., Otto-Bliesner, B.L., Rosenbloom, N., 2012. Causes of early Holocene desertification in arid Central Asia. Clim. Dyn. 38, 1577–1591.
Kalugin, I., Daryin, A., Smolyaninova, L., Andreev, A., Diekmann, B., Khlystov, O., 2007. 800-yr-long records of annual air temperature and precipitation over southern Siberia inferred from Teletskoye Lake sediments. Quat. Res. 67, 400–410.
Karabanov, E.B., Williams, D.F., Kuzmin, M., Sideleva, V., Khursevich, G., Prokopenko, A., Solotchina, E., Tkachenko, L., Fedenya, S., Kerber, E., Gvozdkov, A., Khlustov, O., Bezrukova, E., Letunova, P., Krapivina, S., 2004. Ecological collapse of Lake Baikal and Lake Hovsgol ecosystems during the last Glacial and consequences for aquatic species diversity. Palaeogeogr. Palaeoclimatol. Palaeoecol. 209, 227–243.
Karpychev, Y.A., 2001. Variations in the Caspian Sea level in the historic epoch. Water Resour. 28, 1–14.
Kaspari, S., Mayewski, P., Kang, S., Sneed, S., Hou, S., Hooke, R., Kreutz, K., Introne, D., Handley, M., Maasch, K., Qin, D., Ren, J., 2007. Reduction in northward incursions of the south Asian monsoon since ~1400 AD inferred from a Mt. Everest ice core. Geophys. Res. Lett. 34https://doi.org/10.1029/2007GL030440. L16701.
Kathayat, G., Cheng, H., Sinha, A., Yi, L., Li, X., Zhang, H., Li, H., Ning, Y., Edwards, R.L., 2017. The Indian monsoon variability and civilization changes in the Indian subcontinent. Sci. Adv. 3, e1701296.
Kim, G.S., Choi, I.S., 1987. A preliminary study on long-term variation of unusual climate phenomena during the past 1000 years in Korea. In: Ye, D., Fu, C., Chao, J., Yoshino, M. (Eds.), The Climate of China and Global Climate. China Ocean Press, Beijing, pp. 30–37.
Kroonenberg, S.B., Abdurakhmanov, G.M., Badyukova, E.N., Van der Borg, K., Kalashnikov, A., Kasirnov, N.S., Rychagov, G.I., Svitoch, A.A., Vonhof, H.B., Wesselingh, F.P., 2007. Solar-forced 2600 BP and little ice age highstands of the Caspian Sea. Quat. Int. 173, 137–143.
Kuang, H.C., Zhou, H.D., Hu, J.F., Yang, X.Q., Peng, P.A., Yang, H., 2013. Variations of n-alkanes and compound-specific carbon isotopes in sediment from Huguangyan Maar Lake during the last glacial maximum and Holocene optimum: implications for paleovegetation. Quat. Sci. 33, 1222–1233 (in Chinese with English abstract).
Kuo, T.S., Liu, Z.Q., Li, H.C., Wan, N.J., Shen, C.C., Ku, T.L., 2011. Climate and environmental changes during the past millennium in central western Guizhou, China as recorded by Stalagmite ZJD-21. J. Asian Earth Sci. 40, 1111–1120.
Landmann, G., Reimer, A., Lemcke, G., Kempe, S., 1996. Dating Lateglacial abrupt climate changes in the 14,570 yr long continuous varve record of Lake Van, Turkey. Palaeogeogr. Palaeoclimatol. Palaeoecol. 122, 107–118.
Lauterbach, S., Witt, R., Plessen, B., Dulski, P., Prasad, S., Mingram, J., Gleixner, G., Hettler-Riedel, S., Stebich, M., Schnetger, B., Schwalb, A., 2014. Climatic imprint of the mid-latitude Westerlies in the Central Tian Shan of Kyrgyzstan and teleconnections to North Atlantic climate variability during the last 6000 years. The Holocene 24, 970–984.
Lee, M.K., Lee, Y.I., Lim, H.S., Lee, J.I., Yoon, H.I., 2013. Late Pleistocenee-Holocene records from Lake Ulaan, southern Mongolia: implications for east Asian palaeomonsoonal climate changes. J. Quat. Sci. 28, 370–378.
Lee, H.F., Pei, Q., Zhang, D.D., Choi, K.P., 2015. Quantifying the intra-regional precipitation variability in northwestern China over the past 1,400 years. PLoS One 10, e0131693.
Lei, Y., Tian, L., Bird, B.W., Hou, J., Ding, L., Oimahmadov, I., Gadoev, M., 2014. A 2540-year record of moisture variations derived from lacustrine sediment (Sasikul Lake) on the Pamir Plateau. The Holocene 24, 761–770.
Lei, G., Zhu, Y., Cai, B., Li, Z., Jiang, X., Wu, J., 2017. Mid-late Holocene climate variations in Southeast China inferred by the intermountain peat records from Fujian, China. Quat. Int. 447, 118–127.
Leroy, S.A.G., López-Merino, L., Tudryn, A., Chalié, F., Gasse, F., 2014. Late Pleistocene and Holocene palaeoenvironments in and around the middle Caspian basin as reconstructed from a deep-sea core. Quat. Sci. Rev. 101, 91–110.
Li, J.J., 1990. The patterns of environmental changes since last Pleistocene in northwestern China. Quat. Sci. 3, 197–204 (in Chinese with English abstract).
Li, J.P., Zeng, Q.C., 2003. A new monsoon index and the geographical distribution of the global monsoons. Adv. Atmos. Sci. 20, 299–302.
Li, S.J., Wang, X.T., Xia, W.L., Li, W.C., 2004. The little ice age climate fluctuations derived from lake sediments of Goulucuo, Qinghai-Xizang plateau. Quat. Sci. 24, 578–584 (in Chinese with English abstract).
Li, J.B., Gou, X.H., Cook, E.R., Chen, F.H., 2006. Tree-ring based drought reconstruction for the central Tien Shan area in Northwest China. Geophys. Res. Lett. 33https://doi.org/10.1029/2006GL025803.. L07715.
Li, J.B., Chen, F.H., Cook, E.R., Gou, X.H., Zhang, Y.X., 2007. Drought reconstruction for North Central China from tree rings: the value of the Palmer drought severity index. Int. J. Climatol. 27, 903–909.
Li, X., Zhao, K., Dodson, J., Zhou, X., 2011a. Moisture dynamics in Central Asia for the last 15 kyr: new evidence from Yili Valley, Xinjiang, NW China. Quat. Sci. Rev. 30, 3457–3466.
Li, H.C., Lee, Z.H., Wan, N.J., Shen, C.C., Li, T.Y., Yuan, D.X., Chen, Y.H., 2011b. The $\delta^{18}O$ and $\delta^{13}C$ records in an aragonite stalagmite from Furong Cave, Chongqing, China: a-2000-year record of monsoonal climate. J. Asian Earth Sci. 40, 1121–1130.
Li, D.L., Jiang, H., Li, T.G., Zhao, M.X., 2011c. Late Holocene paleoenvironmental changes in the southern Okinawa Trough inferred from a diatom record. Chin. Sci. Bull. 56, 1131–1138.
Li, B.F., Chen, Y.N., Shi, X., Chen, Z.S., Li, W.H., 2013. Temperature and precipitation changes in different environments in the arid region of Northwest China. Theor. Appl. Climatol. 112, 589–596.
Li, G.Q., Rao, Z.G., Duan, Y.W., Xia, D.S., Wang, L.B., Madsen, D.B., Jia, J., Wei, H.T., Qiang, M.R., Chen, J.H., Chen, F.H., 2016. Paleoenvironmental changes recorded in a luminescence dated loess/paleosol sequence from the Tianshan Mountains, arid Central Asia, since the Penultimate Glaciation. Earth Planet. Sci. Lett. 448, 1–12.
Liang, E., Liu, X., Yuan, Y., Qin, N., Fang, X., Huang, L., Zhu, H., Wang, L., Shao, X., 2006. The 1920s drought recorded by tree rings and historical documents in the semi-arid and arid areas of northern China. Clim. Chang. 79, 403–432.
Linderholm, H.W., Braeuning, A., 2006. Comparison of high-resolution climate proxies from the Tibetan plateau and Scandinavia during the last millennium. Quat. Int. 154, 141–148.
Ling, Y., Dai, X., Zheng, M., Sun, Q., Chu, G., Wang, H., Xie, M., Shan, Y., 2018. High-resolution geochemical record for the last 1100 yr from Lake Toson, northeastern Tibetan Plateau, and its climatic implications. Quat. Int. 487, 61–70.
Liu, B., 1976. Climate Change in Southern Tarim Basin. 1976 Ancient and Present-Day Bookstore, Tokyo.
Liu, K.B., Yao, Z.J., Thompson, L.G., 1998. A pollen record of Holocene climatic changes from the Dunde ice cap, Qinghai-Tibetan Plateau. Geology 26, 135–138.
Liu, Z., Henderson, A.C.G., Huang, Y., 2006. Alkenone-based reconstruction of late-Holocene surface temperature and salinity changes in Lake Qinghai, China. Geophys. Res. Lett. 33https://doi.org/10.1029/2006GL026151. L09707.
Liu, X., Herzschuh, U., Shen, J., Jiang, Q., Xiao, X., 2008. Quat. Res. 70, 412–425 Holocene environmental and climatic changes inferred from Wulungu Lake in northern Xinjiang, China.
Liu, Z.Y., Otto-Bliesner, B., He, F., Brady, E., Clark, P., Lynch-Steiglitz, J., Carlson, A., Curry, W., Brook, E., Jacob, R., Erickson, D., Kutzbach, J., Cheng, J., 2009. Transient simulation of deglacial climate evolution with a new mechanism for Bølling-Allerød warming. Science 325, 310–314.
Liu, W., Liu, Z., An, Z., Wang, X., Chang, H., 2010. Wet climate during the 'Little Ice Age' in the arid Tarim Basin, northwestern China. In: The Holocene. vol. 21. pp. 409–416.
Liu, J., Chen, F., Chen, J., Xia, D., Xu, Q., Wang, Z., Li, Y., 2011. Humid medieval warm period recorded by magnetic characteristics of sediments from Gonghai Lake, Shanxi, North China. Chin. Sci. Bull. 56, 2464–2474.
Liu, J., Wang, B., Cane, M.A., Yim, S.Y., Lee, J.Y., 2013. Divergent global precipitation changes induced by natural versus anthropogenic forcing. Nature 493, 656–659.
Liu, Z.Y., Wen, X.Y., Brady, E.C., Otto-Bliesner, B., Yu, G., Lu, H.Y., Cheng, H., Wang, Y.J., Zheng, W.P., Ding, Y.H., Edwards, R.L., Cheng, J., Liu, W., Yang, H., 2014. Chinese cave records and the East Asia Summer Monsoon. Quat. Sci. Rev. 83, 115–128.
Liu, J., Chen, J., Zhang, X., Li, Y., Rao, Z., Chen, F., 2015. Holocene East Asian summer monsoon records in northern China and their inconsistency with Chinese stalagmite $\delta^{18}O$ records. Earth Sci. Rev. 148, 194–208.
Liu, J., Chen, J., Zhang, X., Chen, S., Liu, X., Huang, W., Chen, F., 2019. Some New Insights on Chinese Cave $\delta^{18}O$ Records and their Paleoclimatic Significance. (in preparation).
Lu, H., Yi, S., Liu, Z., Mason, J.A., Jiang, D., Cheng, J., Stevens, T., Xu, Z., Zhang, E., Jin, L., Zhang, Z., Guo, Z., Wang, Y., Otto-Bliesner, B., 2013. Variation of East Asian monsoon precipitation during the past 21 k.y. and potential CO_2 forcing. Geology 41, 1023–1026.
Ma, J.Z., Edmunds, W.M., 2006. Groundwater and lake evolution in the Badain Jaran desert ecosystem, Inner Mongolia. Hydrogeol. J. 14, 1231–1243.
Ma, Z., Fu, C., 2006. Some evidence of drying trend over northern China from 1951 to 2004. Chin. Sci. Bull. 51, 2913–2925.
Ma, C., Wang, F., Cao, Q., Xia, X., Li, S., Li, X., 2008. Climate and environment reconstruction during the medieval warm period in Lop Nur of Xinjiang. China. Chin. Sci. Bull. 53, 3016–3027.
Maher, B.A., Thompson, R., 2012. Oxygen isotopes from Chinese caves: records not of monsoon rainfall but of circulation regime. J. Quat. Sci. 27, 615–624.
Man, Z.M., 2009. Research on Climate Change during Historical Times in China. Shandong Education Press, Ji'nan.
Marcott, S.A., Shakun, J.D., Clark, P.U., Mix, A.C., 2013. A reconstruction of regional and global temperature for the past 11,300 years. Science 339, 1198–1201.
Mathew, B., Heidi, C., Bradfield, L., 2002. Drought in central and Southwest Asia: La Niña, the warm pool, and Indian Ocean precipitation. J. Clim. 15, 697–700.
Meng, H.W., Ma, Y.Z., Wang, W., Sang, Y.L., 2009. Vegetation and environment change based on high resolution pollen records of the last 2400 years in Dingbian, Shaanxi Province, China. Quat. Sci. 29, 931–942 (in Chinese with English abstract).
Mischke, S., Zhang, C., 2011. Ostracod distribution in Ulungur Lake (Xinjiang, China) and a reassessed Holocene record. Ecol. Res. 26, 133–145.
Müller, C., 2017. Bi-decadal climate reconstruction derived from a 1200-year long pollen record from the NE Qinghai-Tibet Plateau and its implications for discussion of the late Holocene environmental dynamics. Quat. Int. 444, 1–10.
Nara, F., Tani, Y., Soma, Y., Soma, M., Naraoka, H., Watanabe, T., Horiuchi, K., Kawai, T., Oda, T., Nakamura, T., 2005. Response of phytoplankton productivity to climate change recorded by sedimentary photosynthetic pigments in Lake Hovsgol

(Mongolia) for the last 23,000 years. Quat. Int. 136, 71–81.
Narama, C., Kicengge, Kubota, J. Shatravin, Duishonakunov, M., Moholdt, G., Abdrakhmatov, K., 2010. The lake-level changes in Central Asia during the last 1000 years based on historical map. Proceedings of International Workshop on "Reconceptualizing Cultural and Environmental Change in Central Asia: An Historical Perspective on the Future", pp. 11–27.
Neff, U., Burns, S.J., Mangini, A., Mudelsee, M., Fleitmann, D., Matter, A., 2001. Strong coherence between solar variability and the monsoon in Oman between 9 and 6 kyr ago. Nature 411, 290–293.
Otto-Bliesner, B.L., Brady, E.C., Fasullo, J., Jahn, A., Landrum, L., Stevenson, S., Rosenbloom, N., Mai, A., Strand, G., 2016. Climate variability and change since 850 C.E.: an ensemble approach with the Community Earth System Model (CESM). B. AM. Meteorol. Soc. 97, 735–754.
Park, J., Han, J., Jin, Q., Bahk, J., Yi, S., 2017. The link between ENSO-like forcing and hydroclimate variability of coastal East Asia during the last millennium. Sci. Rep. 7, 8166.
Paulsen, D.E., Li, H.C., Ku, T.L., 2003. Climate variability in Central China over the last 1270 years revealed by high-resolution stalagmite records. Quat. Sci. Rev. 22, 691–701.
Peck, J.A., Khosbayar, P., Fowell, S.J., Pearce, R.B., Ariunbileg, S., Hansen, B.C.S., Soninkhishig, N., 2002. Mid to late Holocene climate change in north Central Mongolia as recorded in the sediments of Lake Telmen. Palaeogeogr. Palaeoclimatol. Palaeoecol. 183, 135–153.
Pederson, N., Hessl, A.E., Baatarbileg, N., Anchukaitis, K.J., Di Cosmo, N., 2014. Pluvials, droughts, the Mongol Empire, and modern Mongolia. Proc. Natl. Acad. Sci. U. S. A. 111, 4375–4379.
Prokopenko, A.A., Kuzmin, M.I., Williams, D.F., Gelety, V.F., Kalmychkov, G.V., Gvozdkov, A.N., Solotchin, P.A., 2005. Basin-wide sedimentation changes and deglacial lake-level rise in the Hovsgol basin, NW Mongolia. Quat. Int. 136, 59–69.
Pu, Y., Nace, T., Meyers, P.A., Zhang, H., Wang, Y., Zhang, C.L., Shao, X., 2013. Paleoclimate changes of the last 1000-yr on the eastern Qinghaie Tibetan Plateau recorded by elemental, isotopic, and molecular organic matter proxies in sediment from glacial Lake Ximencuo. Palaeogeogr. Palaeoclimatol. Palaeoecol. 379–380, 39–53.
Putnam, A.E., Putnam, D.E., Andreu-Hayles, L., Cook, E.R., Palmer, J.G., Clark, E.H., Wang, C., Chen, F., Denton, G.H., Boyle, D.P., Bassett, S.D., 2016. Little Ice Age wetting of interior Asian deserts and the rise of the Mongol Empire. Quat. Sci. Rev. 131, 33–50.
Qian, W.H., Qin, A., 2008. Precipitation division and climate shift in China from 1960 to 2000. Theor. Appl. Climatol. 93, 1–17.
Rasmussen, K.A., Ricketts, R.D., Johnson, T.C., Romanovsky, V.V., Grigina, O.M., 2001. An 8,000 Year Multi-Proxy Record from Lake Issyk-Kul, Kyrgyzstan. 9. PAGES News, pp. 5–6.
Ren, G.Y., 1998. Pollen evidence for increased summer rainfall in the medieval warm period at Maili, Northeast China. Geophys. Res. Lett. 25, 1931–1934.
Ricketts, R.D., Johnson, T.C., Brown, E.T., Rasmussen, K.A., Romanovsky, V.V., 2001. The Holocene paleolimnology of Lake Issyk-Kul, Kyrgyzstan: trace element and stable isotope composition of ostracodes. Palaeogeogr. Palaeoclimatol. Palaeoecol. 176, 207–227.
Rogers, J.C., Van, L.H., 1979. The seesaw in winter temperatures between Greenland and Northern Europe. Part II: some oceanic and atmospheric effects in middle and high latitudes. Mon. Weather Rev. 107, 509–519.
Rossby, C.G., 1939. Relation between variations in the intensity of the zonal circulation of the atmosphere and the displacements of the semi-permanent centers of action. J. Mar. Res. 2, 38–55.
Sanwal, J., Kotlia, B.S., Rajendran, C., Ahmad, S.M., Rajendran, K., Sandiford, M., 2013. Climatic variability in Central Indian Himalaya during the last ~1800 years: evidence from a high resolution speleothem record. Quat. Int. 304, 183–192.
Shao, X.M., Huang, L., Liu, H.B., Liang, E.Y., Fang, X.Q., Wang, L.L., 2005. Reconstruction of precipitation variation from tree rings in recent 1000 years in Delingha, Qinghai. Sci. China Ser. D 48, 939–949.
Shen, J., Liu, X.Q., Wang, S.M., Ryo, M., 2005. Palaeoclimatic changes in the Qinghai Lake area during the last 18,000 years. Quat. Int. 136, 131–140.
Sheng, E., Yu, K., Xu, H., Lan, J., Liu, B., Che, S., 2015. Late holocene Indian summer monsoon precipitation history at Lake Lugu, northwestern Yunnan Province, southwestern China. Palaeogeogr. Palaeoclimatol. Palaeoecol. 438, 24–33.
Shi, Y.F., Shen, Y.P., Kang, E., Li, D.L., Ding, Y.J., Zhang, G.W., Hu, R.J., 2007. Recent and future climate change in Northwest China. Clim. Chang. 80, 379–393.
Shi, J., Yan, Q., Jiang, D.B., Min, J.Z., Jiang, Y., 2016. Precipitation variation over eastern China and arid Central Asia during the past millennium and its possible mechanism: Perspectives from PMIP3 experiments. J. Geophys. Res. Atmos. 121, 11989–12004.
Sinha, A., Berkelhammer, M., Stott, L., Mudelsee, M., Cheng, H., Biswas, J., 2011. The leading mode of Indian summer monsoon precipitation variability during the last millennium. Geophys. Res. Lett. 38, L15703 doi: https://doi.org/10.1029/2011GL047713.
Sinha, A., Kathayat, G., Cheng, H., Breitenbach, S.F., Berkelhammer, M., Mudelsee, M., Biswas, J., Edwards, R.L., 2015. Trends and oscillations in the Indian summer monsoon rainfall over the last two millennia. Nat. Commun. 6, 6309.
Song, M., Zhou, A., Zhang, X., Zhao, C., He, Y., Yang, W., Liu, W., Li, S., Liu, Z., 2015. Solar imprints on Asian inland moisture fluctuations over the last millennium. The Holocene 25, 1935–1943.
Sorrel, P., Popescu, S.M., Head, M.J., Suc, J.P., Klotz, S., Oberhansli, H., 2006. Hydrographic development of the Aral Sea during the last 2000 years based on a quantitative analysis of dinoflagellate cysts. Palaeogeogr. Palaeoclimatol. Palaeoecol. 234, 304–327.
Sun, A., Feng, Z., Ran, M., Zhang, C., 2013. Pollen-recorded bioclimatic variations of the last ~22,600 years retrieved from Achit Nuur core in the western Mongolian Plateau. Quat. Int. 311, 36–43.
Tan, M., 2014. Circulation effect: response of precipitation $\delta^{18}O$ to the ENSO cycle in monsoon regions of China. Clim. Dyn. 42, 1067–1077.
Tan, L.C., Cai, Y.J., Yi, L., An, Z.S., Ai, L., 2008. Precipitation variations of Longxi, northeast margin of Tibetan Plateau since AD 960 and their relationship with solar activity. Clim. Past 4, 19–28.
Tan, L.C., Cai, Y.J., An, Z.S., Edwards, R.L., Cheng, H., Shen, C.C., Zhang, H.W., 2011. Centennial-to decadal-scale monsoon precipitation variability in the semi-humid region, northern China during the last 1860 years: Records from stalagmites in Huangye Cave. The Holocene 21, 287–296.
Tan, L., Cai, Y., Cheng, H., Edwards, L.R., Lan, J., Zhang, H., Li, D., Ma, L., Zhao, P., Gao, Y., 2018. High resolution monsoon precipitation changes on southeastern Tibetan Plateau over the past 2300 years. Quat. Sci. Rev. 195, 122–132.
Tao, S.C., An, C.B., Chen, F.H., Tang, L.Y., Wang, Z.L., Lü, Y.B., Li, Z.F., Zheng, T.M., Zhao, J.J., 2010. Pollen-inferred vegetation and environmental changes since 16.7 ka BP at Balikun Lake, Xinjiang. Chin. Sci. Bull. 55, 2449–2457.
Tarasov, P.E., Pushenko, M.Ya., Harrison, S.P., Saarse, L., Andreev, A.A., Aleshinskaya, Z.V., Davydova, N.N., Dorofeyuk, N.I., Efremov, Yu.V., Elina, G.A., Elovicheva, Ya.K., Filimonova, L.V., Gunova, V.S., Khomutova, V.I., Kvavadze, E.V., Neustrueva, I.Yu., Pisareva, V.V., Sevastyanov, D.V., Shelekhova, T.S., Subetto, D.A., Uspenskaya, O.N., Zernitskaya, V.P., 1996. Lake status records from the former Soviet Union and Mongolia: documentation of the second version of the data base. In: NOAA Paleoclimatology Publications Series Report No. 5, (Boulder, CO).
Thompson, L.G., Mosley-Thompson, E., Davis, M.E., Lin, P.E., Henderson, K.A., Cole-Dai, J., Bolzan, J.F., Liu, K.B., 1995. A 1000 year climate ice-core record from the Guliya ice cap, China: its relationship to global climate variability. Ann. Glaciol. 21, 175–181.
Tian, F., Herzschuh, U., Dallmeyer, A., Xu, Q., Mischke, S., Biskaborn, B.K., 2013. Environmental variability in the monsoon-westerlies transition zone during the last 1200 years: lake sediment analyses from Central Mongolia and supra-regional synthesis. Quat. Sci. Rev. 73, 31–47.
Tong, G.B., Zhang, J.P., Fan, S.X., Zhao, J.B., Wang, G.H., Wang, Y.H., Wang, L.X., Cui, J., 1996. Environment changes at the top of Taibai Mountain, Qinling since 1ka ago. Mar. Geol. Quat. Geol. 16, 95–104 (in Chinese with English abstract).
Tong, G.B., Shi, Y., Wu, R.J., Yang, X.D., Qu, W.C., 1997. Vegetation and climatic quantitative reconstruction of Longgan Lake since the past 3000 years. Mar. Geol. Quat. Geol. 17, 53–61 (in Chinese with English abstract).
Treydte, K.S., Schleser, G.H., Helle, G., Frank, D.C., Winiger, M., Haug, G.H., Esper, J., 2006. The twentieth century was the wettest period in northern Pakistan over the past millennium. Nature 440, 1179–1182.
Uno, I., Eguchi, K., Yumimoto, K., Takemura, T., Shimizu, A., Uematsu, M., Liu, Z., Wang, Z., Hara, Y., Sugimoto, N., 2009. Asian dust transported one full circuit around the globe. Nat. Geosci. 2, 557–560.
von Rad, U., Schaaf, M., Michels, K.H., Schulz, H., Berger, W.H., Sirocko, F., 1999. A 5000-yr record of climate change in varved sediments from the oxygen minimum zone off Pakistan, Northeastern Arabian Sea. Quat. Res. 51, 39–53.
Wang, H.J., 2001. The weakening of the Asian Monsoon circulation after the end of 1970's. Adv. Atmos. Sci. 18, 376–386.
Wang, H.J., Chen, H.P., 2012. Climate control for southeastern China moisture and precipitation: Indian or East Asian monsoon? J. Geophys. Res. 117https://doi.org/10.1029/2012JD017734. D12109.
Wang, B., Ding, Q.H., 2006. Changes in global monsoon precipitation over the past 56 years. Geophys. Res. Lett. 33, L06711. https://doi.org/10.1029/2005GL025347.
Wang, W., Feng, Z.D., 2013. Holocene moisture evolution across the Mongolian Plateau and its surrounding areas: a synthesis of climatic records. Earth Sci. Rev. 122, 38–57.
Wang, S.M., Ji, L., 1995. Deposits and history of Lake level fluctuation in Hulun Lake. J. Lake Sci. 7, 297–308 (in Chinese with English abstract).
Wang, W.G., Feng, Z.D., Lee, X.Q., Zhang, H.C., An, C.B., Guo, L.L., 2004. Holocene abrupt climate shifts recorded in Gun Nuur lake core, northern Mongolia. Chin. Sci. Bull. 49, 520–526.
Wang, Y.J., Cheng, H., Edwards, R.L., He, Y.Q., Kong, X.G., An, Z.S., Wu, J.Y., Kelly, M.J., Dykoski, C.A., Li, X.D., 2005. The Holocene Asian monsoon: links to solar changes and North Atlantic climate. Science 308, 854–857.
Wang, W., Feng, Z.D., Ran, M., Zhang, C.J., 2013a. Holocene climate and vegetation changes inferred from pollen records of Lake Aibi, northern Xinjiang, China: a potential contribution to understanding of Holocene climate pattern in Eastcentral Asia. Quat. Int. 311, 54–62.
Wang, W.Z., Liu, X.H., Xu, G.B., Shao, X.M., Qin, D.H., Sun, W.Z., An, W.L., Zeng, X.M., 2013b. Moisture variations over the past millennium characterized by Qaidam Basin tree-ring $\delta^{18}O$. Chin. Sci. Bull. 58, 3956–3961.
Wang, L.C., Behling, H., Lee, T.Q., Li, H.C., Huh, C.A., Shiau, L.J., Chen, S.H., Wu, J.T., 2013c. Increased precipitation during the little ice age in northern Taiwan inferred from diatoms and geochemistry in a sediment core from a subalpine lake. J. Paleolimnol. 49, 619–631.
Wang, P.X., Wang, B., Cheng, H., Fasullo, J., Guo, Z., Kiefer, T., Liu, Z., 2017. The global monsoon across time scales: Mechanisms and outstanding issues. Earth Sci. Rev. 174, 84–121.
Wei, K., Gasse, F., 1999. Oxygen isotopes in lacustrine carbonates of West China revisited: implications for post glacial changes in summer monsoon circulation. Quat. Sci. Rev. 18, 1315–1334.
Wei, W., Zhang, R.H., Wen, M., Rong, X.Y., Li, T., 2014. Impact of Indian summer monsoon on the South Asian High and its influence on summer rainfall over China. Clim. Dyn. 43, 1257–1269.
Wei, W., Zhang, R.H., Wen, M., Kim, B.-J., Nam, J.-C., 2015. Interannual Variation of the South Asian High and its Relation with Indian and East Asian Summer Monsoon

Rainfall. J. Clim. 28, 2623–2634.
Wick, L., Lemcke, G., Sturm, M., 2003. Evidence of Lateglacial and Holocene climatic change and human impact in eastern Anatolia: high-resolution pollen, charcoal, isotopic and geochemical records from the laminated sediments of Lake Van, Turkey. The Holocene 13, 665–675.
Wu, J.L., Liu, J.J., Wang, S.M., 2004. Climate change record from stable isotopes in Lake Aibi, Xinjiang during the past 1500 years. Quat. Sci. 24, 585–590 (in Chinese with English abstract).
Wünnemann, B., Chen, F.H., Riedel, F., Zhang, C.J., Chen, G.J., Demske, D., Jin, M., 2003. Holocene Lake deposits of Bosten Lake, southern Xinjiang, China. Chin. Sci. Bull. 48, 1429–1432.
Wünnemann, B., Mischke, S., Chen, F.H., 2006. A Holocene sedimentary record from Bosten Lake, China. Palaeogeogr. Palaeoclimatol. Palaeoecol. 234, 223–238.
Xiao, J.L., Xu, Q.H., Nakamura, T., Yang, X.L., Liang, W.D., Inouchi, Y., 2004. Holocene vegetation variation in the Daihai Lake region of north–Central China: a direct indication of the Asian monsoon climatic history. Quat. Sci. Rev. 23, 1669–1679.
Xiao, J., Si, B., Zhai, D., Itoh, S., Lomtatidze, Z., 2008. Hydrology of Dali Lake in central-eastern Inner Mongolia and Holocene East Asian monsoon variability. J. Paleolimnol. 40, 519–528.
Xiao, X., Haberle, S.G., Shen, J., Yang, X., Han, Y., Zhang, E., Wang, S., 2014. Latest Pleistocene and Holocene vegetation and climate history inferred from an alpine lacustrine record, northwestern Yunnan Province, southwestern China. Quat. Sci. Rev. 86, 35–48.
Xu, Q.H., Xiao, J.L., Li, Y.C., Tian, F., Nakagawa, T., 2010. Pollen-based quantitative reconstruction of Holocene climate changes in the Daihai Lake area, Inner Mongolia, China. J. Clim. 23, 2856–2868.
Xue, J., Zhong, W., 2011. Holocene climate variation denoted by Barkol Lake sediments in northeastern Xinjiang and its possible linkage to the high and low latitude climates. Sci. China Earth Sci. 54, 603–614.
Yadava, A.K., Braeuning, A., Singh, J., Yadav, R.R., 2016. Boreal spring precipitation variability in the cold arid western Himalaya during the last millennium, regional linkages, and socio-economic implications. Quat. Sci. Rev. 144, 28–43.
Yan, H., Sun, L., Oppo, D.W., Wang, Y., Liu, Z., Xie, Z., Liu, X., Cheng, W., 2011. South China Sea hydrological changes and Pacific Walker Circulation variations over the last millennium. Nat. Commun. 2, 293.
Yang, X.D., Wang, S.M., 1996. The vegetational and climatic-environmental changes in Hulun Lake and Wulungu Lake during Holocene. Oceanol. Limnol. Sin. 27, 67–72 (in Chinese with English abstract).
Yang, X.P., Zhu, Z.D., Jaekel, D., Owen, L.A., Han, J.M., 2002. Late Quaternary palaeoenvironment change and landscape evolution along the Keriya River, Xinjiang, China: the relationship between high mountain glaciation and landscape evolution in foreland desert regions. Quat. Int. 97, 155–166.
Yang, S.L., Ding, F., Ding, Z., 2006a. Pleistocene chemical weathering history of Asian arid and semi-arid regions recorded in loess deposits of China and Tajikistan. Geochim. Cosmochim. Acta 70, 1695–1709.
Yang, X., Liu, Z., Zhang, F., White, P.D., Wang, X., 2006b. Land Degrad. Dev. 17, 381–392 Hydrological changes and land degradation in the southern and eastern Tarim basin, Xinjiang, China.
Yang, B., Wang, J., Bräuning, A., Dong, Z., Esper, J., 2009. Late Holocene climatic and environmental changes in arid Central Asia. Quat. Int. 194, 68–78.
Yang, B., Qin, C., Shi, F., Sonechkin, D.M., 2012. Tree ring-based annual streamflow reconstruction for the Heihe River in arid northwestern China from AD 575 and its implications for water resource management. The Holocene 22, 773–784.
Yang, B., Qin, C., Wang, J., He, M., Melvin, T.M., Osborn, T.J., Briffa, K.R., 2014. A 3,500-year tree-ring record of annual precipitation on the northeastern Tibetan Plateau. Proc. Natl. Acad. Sci. U. S. A. 111, 2903–2908.
Yao, T.D., Qin, D.H., Tian, L.D., Jiao, K.Q., Yang, Z.H., Xie, C., 1996. Variations in temperature and precipitation in the past 2000 a on the Xizang (Tibet) Plateau–Guliya ice core record. Sci. China Ser. D 39, 425–433.
Yu, G., Xue, B., Wang, S.M., Liu, J., 2000. Lake records and LGM climate in China. Chin. Sci. Bull. 45, 1158–1164.
Zhang, X.J., Jin, L.Y., 2016. Association of the Northern Hemisphere circumglobal teleconnection with the Asian summer monsoon during the Holocene in a transient simulation. The Holocene 26, 290–301.
Zhang, Z.K., Wu, R.J., Wang, S.M., Xia, W.L., Wu, Y.H., Qu, W.C., 1998. Environmental changes recorded by Lake sediments from East Juyanhai Lake in Inner Mongolia during the past 2600 years. J. Lake Sci. 10, 44–51 (in Chinese with English abstract).
Zhang, P.Z., Cheng, H., Edwards, R.L., Chen, F.H., Wang, Y.J., Yang, X.L., Liu, J., Tan, M., Wang, X.F., Liu, J.H., An, C.L., Dai, Z.B., Zhou, J., Zhang, D.Z., Jia, J.H., Jin, L.Y., Johnson, K.R., 2008. A test of climate, sun, and culture relationships from an 1810-year Chinese cave record. Science 322, 940–942.
Zhang, Y., Kong, Z.C., Yan, S., Yang, Z.J., Ni, J., 2009. “Medieval warm period” on the northern slope of central Tianshan mountains, Xinjiang, NW China. Geophys. Res. Lett. 36https://doi.org/10.1029/2009gl037375. L11702.
Zhang, Y., Tian, Q.H., Gou, X.H., Chen, F.H., Leavitt, S.W., Wang, Y.S., 2011. Annual precipitation reconstruction since AD 775 based on tree rings from the Qilian Mountains, northwestern China. Int. J. Climatol. 31, 371–381.
Zhang, C., Zhang, W., Feng, Z., Mischke, S., Gao, X., Gao, D., Sun, F., 2012. Holocene hydrological and climatic change on the northern Mongolian Plateau based on multi-proxy records from Lake Gun Nuur. Palaeogeogr. Palaeoclimatol. Palaeoecol. 323–325, 75–86.
Zhang, B.Q., He, C.S., Burnham, M., Zhang, L.H., 2016a. Evaluating the coupling effects of climate aridity and vegetation restoration on soil erosion over the Loess Plateau in China. Sci. Total Environ. 539, 436–449.
Zhang, X.J., Jin, L.Y., Huang, W., Chen, F.H., 2016b. Forcing mechanisms of obtial-scale changes in winter rainfall over northwestern China during the Holocene. The Holocene 26, 549–555.
Zhao, Y., Yu, Z.C., Liu, X.J., Zhao, C., Chen, F.H., Zhang, K., 2010. Late Holocene vegetation and climate oscillations in the Qaidam Basin of the northeastern Tibetan Plateau. Quat. Res. 73, 59–69.
Zhao, Z.L., Wang, Y., Yao, P.Y., Chi, Z.Q., Guan, Y.Y., 2011. Environmental changes recorded by lacustrine sediments since late Holocene in Central Inner Mongolia. Geol. Bull. China 30, 1251–1255 (in Chinese with English abstract).
Zhao, Y.T., An, C.B., Mao, L.M., Zhao, J.J., Tang, L.Y., Zhou, A.F., Li, H., Dong, W.M., Duan, F.T., Chen, F.H., 2015. Vegetation and climate history in arid western China during MIS2: New insights from pollen and grain-size data of the Balikun Lake, eastern Tien Shan. Quat. Sci. Rev. 126, 112–125.
Zheng, J.Y., Wang, W.C., Ge, Q.S., Man, Z.M., Zhang, P.Y., 2006. Precipitation variability and extreme events in eastern China during the past 1500 years. Terr. Atmos. Ocean. Sci. 17, 579–592.
Zhong, W., Xiong, H.G., 1999. Paleo-climatic and environmental development since about 4 ka B.P. And the relation with abandonments of ancient cities in Southern Xinjiang. J. Desert Res. 19, 343–347 (in Chinese with English abstract).
Zhou, A.F., Sun, H.L., Chen, F.H., Zhao, Y., An, C.B., Dong, G.H., Wang, Z.L., Chen, J.H., 2010. High-resolution climate change in mid-late Holocene on Tianchi Lake, Liupan Mountain in the Loess Plateau in Central China and its significance. Chin. Sci. Bull. 55, 2118–2121.
Zhou, X.J., Zhao, P., Liu, G., Zhou, T.J., 2011. Characteristics of decadal-centennial-scale changes in East Asian summer monsoon circulation and precipitation during the medieval warm period and Little Ice Age and in the present day. Chin. Sci. Bull. 56, 3003–3011.